

REPORT DOCUMENTATION PAGE

Form Approved
OMB No. 0704-0188

The public reporting burden for this collection of information is estimated to average 1 hour per response, including the time for reviewing instructions, searching existing data sources, gathering and maintaining the data needed, and completing and reviewing the collection of information. Send comments regarding this burden estimate or any other aspect of this collection of information, including suggestions for reducing the burden, to the Department of Defense, Executive Services and Communications Directorate (0704-0188). Respondents should be aware that notwithstanding any other provision of law, no person shall be subject to any penalty for failing to comply with a collection of information if it does not display a currently valid OMB control number.

PLEASE DO NOT RETURN YOUR FORM TO THE ABOVE ORGANIZATION.

1. REPORT DATE (DD-MM-YYYY) 30-05-2013	2. REPORT TYPE Journal Article	3. DATES COVERED (From - To)
---	-----------------------------------	------------------------------

4. TITLE AND SUBTITLE A 1-D simulation analysis of the development and maintenance of the 2001 red tide of the ichthyotoxic dinoflagellate <i>Karenia brevis</i> on the West Florida shelf	5a. CONTRACT NUMBER
	5b. GRANT NUMBER
	5c. PROGRAM ELEMENT NUMBER 0602435N

6. AUTHOR(S) J.M. Lenes, B.P. Darrow, J.J. Walsh, J.K. Jolliff, F.R. Chen, R.H. Weisberg, L. Zheng	5d. PROJECT NUMBER
	5e. TASK NUMBER
	5f. WORK UNIT NUMBER 73-6463-01-5

7. PERFORMING ORGANIZATION NAME(S) AND ADDRESS(ES) Naval Research Laboratory Oceanography Division Stennis Space Center, MS 39529-5004	8. PERFORMING ORGANIZATION REPORT NUMBER NRL/JA/7330-11-798
---	--

9. SPONSORING/MONITORING AGENCY NAME(S) AND ADDRESS(ES) Office of Naval Research One Liberty Center 875 North Randolph Street, Suite 1425 Arlington, VA 22203-1995	10. SPONSOR/MONITOR'S ACRONYM(S) ONR
	11. SPONSOR/MONITOR'S REPORT NUMBER(S)

12. DISTRIBUTION/AVAILABILITY STATEMENT
Approved for public release, distribution is unlimited.

13. SUPPLEMENTARY NOTES

14. ABSTRACT
A one-dimensional (1-D) ecological model, HABSIM, examined the initiation and maintenance of the 2001 red tide on the West Florida shelf (WFS). Phytoplankton competition among toxic dinoflagellates (*Karenia brevis*), nitrogen fixing cyanophytes (*Trichodesmium erythraeum*), large siliceous phytoplankton (diatoms), and small non-siliceous phytoplankton (microflagellates) explored the sequence of events required to support the observed red tide from August to December 2001. The ecological model contained 24 state variables within five submodels: circulation, atmospheric (iron deposition), bio-optics, pelagic (phytoplankton, nutrients, bacteria, zooplankton, and fish), and benthic (nutrient regeneration). The 2001 model results reaffirmed that diazotrophs are the basis for initiation of red tides of *K. brevis* on the WFS. A combination of selective grazing pressure, iron fertilization, low molar nitrogen to phosphorus ratios, and eventual silica limitation of fast-growing diatoms set the stage for dominance of nitrogen fixers. "New" nitrogen was made available for subsequent blooms of *K. brevis* through the release of ammonium and urea during nitrogen fixation, as well as during cell lysis, by the *Trichodesmium* population. Once *K. brevis* biomass reached ichthyotoxic levels, rapid decay of subsequent fish kills supplied additional organic nutrients for utilization by these opportunistic toxic algae. Both nutrient vectors represented organic non-siliceous sources of nitrogen and phosphorus, further exacerbating silica limitation of the diatom population. The model reproduced this spring transition from a simple estuarine-driven, diatom-based food chain to a complex summer-fall system of *Trichodesmium* and toxic dinoflagellates. While the model was able to replicate the initiation and maintenance of the 2001 red tide, bloom termination was not captured by this 1-D form on the WFS. Here, horizontal advection and perhaps cell lysis loss terms might play a significant role, to be addressed in future three-dimensional simulations.

15. SUBJECT TERMS
Red tide, Harmful algae, *Karenia brevis*, Ecological modeling, West Florida shelf

16. SECURITY CLASSIFICATION OF:			17. LIMITATION OF ABSTRACT UU	18. NUMBER OF PAGES 19	19a. NAME OF RESPONSIBLE PERSON Jason K. Jolliff
a. REPORT Unclassified	b. ABSTRACT Unclassified	c. THIS PAGE Unclassified			19b. TELEPHONE NUMBER (Include area code) (228) 688-5308

PUBLICATION OR PRESENTATION RELEASE REQUEST

Pubkey: 7561

NRLINST 5600.2

Ref: (a) NRL Instruction 5600.2 (b) NRL Instruction 5510.40D	() Abstract only, published () Book () Conference Proceedings (refereed)	() Abstract only, not published () Book chapter () Conference Proceedings (not refereed)	STRN <u>NRLJA/7330-11-798</u>
Encl: (1) Two copies of subject paper (or abstract)	() Invited speaker (X) Journal article (refereed) () Oral Presentation, published () Other, explain	() Multimedia report () Journal article (not refereed) () Oral Presentation, not published	Route Sheet No. <u>7330/</u> Job Order No. <u>73-6463-01-5</u> Classification <u>X</u> U <u> </u> C Sponsor <u>ONR</u> approval obtained <u> </u> yes <u>X</u> no

Title of Paper or Presentation
A 1- D Simulation Analysis of the Development and Maintenance of the 2001 Red Tide of the Ichthyotoxic Dinoflagellate Karenia Brevis on the West F

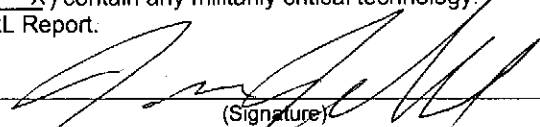
Author(s) Name(s) (First, MI, Last), Code, Affiliation if not NRL
Univ. S. FL
J.M. Lenes Associated Author **B.P. Darrow** Univ. of S. Florida **J.J. Walsh** Associated Author **Jason K Jolliff** 7331 **Feng Chen** Univ. of S. Florida
Robert Weisberg Associated Author **L. Zheng** Univ. of S. Florida
Univ. of S. FL

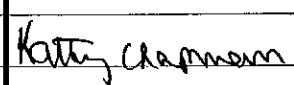
It is intended to offer this paper to the _____
 (Name of Conference)

 (Date, Place and Classification of Conference)

and/or for publication in **Continental Shelf Research, Unclassified**
 (Name and Classification of Publication) (Name of Publisher)

After presentation or publication, pertinent publication/presentation data will be entered in the publications data base, in accordance with reference (a).
 It is the opinion of the author that the subject paper (is _____) (is not X) classified, in accordance with reference (b).
 This paper does not violate any disclosure of trade secrets or suggestions of outside individuals or concerns which have been communicated to the Laboratory in confidence. This paper (does _____) (does not X) contain any militarily critical technology.
 This subject paper (has _____) (has never X) been incorporated in an official NRL Report.

Jason K Jolliff, 7331
 Name and Code (Principal Author)  (Signature)

CODE	SIGNATURE	DATE	COMMENTS
Author(s) Jolliff		8/16/11	Need by <u>31 Aug 11</u> Publicly accessible sources used for this publication
Section Head Gould		8/16/11	
Branch Head Robert A Arnone, 7330	FOR	8/16/11	
Division Head Ruth H. Preller, 7300		8/17/11	1. Release of this paper is approved. 2. To the best knowledge of this Division, the subject matter of this paper (has _____) (has never <u>X</u>) been classified.
Security, Code 1231			1. Paper or abstract was released. 2. A copy is filed in this office.
Office of Counsel, Code 1008.3		8/24/11	
ADOR/Director NCST E. R. Franchi, 7000			
Public Affairs (Unclassified/ Unlimited Only), Code 7030.4		8-23-11	
Division, Code			
Author, Code			

11-1226-3190

PUBLICATION OR PRESENTATION RELEASE REQUEST

Pub. Form 7561 NPLINST 5002

Ref: (a) NRL Instruction 5000.2 (b) NRL Instruction 5510.400	<input type="checkbox"/> Abstract only, published <input type="checkbox"/> Book <input type="checkbox"/> Conference Proceedings (referenced) <input type="checkbox"/> Invited speaker <input checked="" type="checkbox"/> Journal article (referenced) <input type="checkbox"/> Oral Presentation, published <input type="checkbox"/> Other, explain:	<input type="checkbox"/> Abstract only, not published <input type="checkbox"/> Book chapter <input type="checkbox"/> Conference Proceedings (not referenced) <input type="checkbox"/> Multimedia report <input type="checkbox"/> Journal article (not referenced) <input type="checkbox"/> Oral Presentation, not published	STRN <u>NRLDA7330-11-798</u> Route Sheet No. <u>7330</u> Job Order No. <u>73-6443-01-5</u> Classification <u>X</u> Sponsor <u>OHR</u> approval obtained <u>36</u> <u>6</u> <u>MT</u>
End: (1) Two copies of subject paper (or abstract)			

Title of Paper or Presentation
A 1-D Simulation Analysis of the Development and Maintenance of the 2001 Red Tide of the Ichthyotoxic Dinoflagellate *Karreriella Brevis* on the West F

Author(s) Name(s) (First, Middle, Last), Code, Affiliation (if not NRL)
 J.M. Lomas Associated Author B.P. Darrow Univ. of S. Florida J.J. Walsh Associated Author Jason K Jolliff 7331 Feng Chen Univ. of S. Florida
 Robert Weisberg Associated Author L. Zhang Univ. of S. Florida
Univ. of S. FL

It is intended to offer this paper to the _____
 (Name of Conference)

 (Date, Place and Classification of Conference)

and/or for publication in **Continental Shelf Research, Unclassified**
 (Name and Classification of Publication) _____ (Name of Publisher)

After presentation or publication, pertinent publication/presentation data will be entered in the publications data base, in accordance with reference (a).
 It is the opinion of the author that the subject paper (is _____) (is not) classified, in accordance with reference (b).
 This paper does not violate any disclosure of trade secrets or suggestions of outside individuals or concerns which have been communicated to the Laboratory in confidence. This paper (does _____) (does not) contain any military critical technology.
 This subject paper (has _____) (has never) been incorporated in an official NRL Report.

Jason K Jolliff, 7331
 Name and Code (Principal Author) _____ (Signature)

CODE	SIGNATURE	DATE	COMMENTS
Author(s) Jolliff	<i>J. Jolliff</i>	8/16/11	Need by <u>28 Aug 11</u> Publicly accessible sources used for this publication
Secron Head Gould	<i>R. Gould</i>	8/16/11	This is a Final Security Review. Any changes made in the document after approved by Code 1226 nullify the Security Review
Branch Head Robert A. Amons, 7330	<i>R. Gould FOR</i>	8/16/11	
Division Head Ruth H. Prellier, 7300	<i>Ruth H. Prellier</i>	8/17/11	1. Release of this paper is approved. 2. To the best knowledge of this Division, the subject matter of this paper (has _____) (has never <input checked="" type="checkbox"/>) been classified.
Security, Code 1231	<i>Michelle Cicala</i>	8/19/11	1. Paper or abstract was released. 2. A copy is filed in this office.
Office of Counsel, Code 1008.3	<i>Kathy Chammom</i>	8/24/11	Personally identifying emails may not be posted to Publicly accessible DON websites per SECNAVINST 5720.47B encl (1); 3.d. (7)
ADOR, Director NCST E. R. Francis, 7000			
Public Affairs (Unclassified/ Unlimited Only), Code 7030.4	<i>Shannon Ireland</i>	8-23-11	
Division, Code			
Author, Code			

F S



A 1-D simulation analysis of the development and maintenance of the 2001 red tide of the ichthyotoxic dinoflagellate *Karenia brevis* on the West Florida shelf

J.M. Lenés^{a,*}, B.P. Darrow^a, J.J. Walsh^a, J.K. Jolliff^b, F.R. Chen^a, R.H. Weisberg^a, L. Zheng^a

^a College of Marine Science, University of South Florida, St. Petersburg, FL 33701, USA

^b Naval Research Laboratory, Stennis Space Center, MS 39529, USA

ARTICLE INFO

Article history:

Received 5 May 2011

Received in revised form

17 January 2012

Accepted 13 April 2012

Available online 26 April 2012

Keywords:

Red tide

Harmful algae

Karenia brevis

Ecological modeling

West Florida shelf

ABSTRACT

A one-dimensional (1-D) ecological model, HABSIM, examined the initiation and maintenance of the 2001 red tide on the West Florida shelf (WFS). Phytoplankton competition among toxic dinoflagellates (*Karenia brevis*), nitrogen fixing cyanophytes (*Trichodesmium erythraeum*), large siliceous phytoplankton (diatoms), and small non-siliceous phytoplankton (microflagellates) explored the sequence of events required to support the observed red tide from August to December 2001. The ecological model contained 24 state variables within five submodels: circulation, atmospheric (iron deposition), bio-optics, pelagic (phytoplankton, nutrients, bacteria, zooplankton, and fish), and benthic (nutrient regeneration). The 2001 model results reaffirmed that diazotrophs are the basis for initiation of red tides of *K. brevis* on the WFS. A combination of selective grazing pressure, iron fertilization, low molar nitrogen to phosphorus ratios, and eventual silica limitation of fast-growing diatoms set the stage for dominance of nitrogen fixers. “New” nitrogen was made available for subsequent blooms of *K. brevis* through the release of ammonium and urea during nitrogen fixation, as well as during cell lysis, by the *Trichodesmium* population. Once *K. brevis* biomass reached ichthyotoxic levels, rapid decay of subsequent fish kills supplied additional organic nutrients for utilization by these opportunistic toxic algae. Both nutrient vectors represented organic non-siliceous sources of nitrogen and phosphorus, further exacerbating silica limitation of the diatom population. The model reproduced this spring transition from a simple estuarine-driven, diatom-based food chain to a complex summer–fall system of *Trichodesmium* and toxic dinoflagellates. While the model was able to replicate the initiation and maintenance of the 2001 red tide, bloom termination was not captured by this 1-D form on the WFS. Here, horizontal advection and perhaps cell lysis loss terms might play a significant role, to be addressed in future three-dimensional simulations.

© 2012 Elsevier Ltd. All rights reserved.

1. Introduction

Harmful algal blooms (HABs) of the toxic dinoflagellate, *Karenia brevis*, occur annually along the West Florida coast (Steidinger et al., 1998) with far-field implications for both the South Atlantic Bight and northern Gulf of Mexico (Walsh et al., 2006). Origins of these red tide blooms have been traced to bottom initiation along the 20–30 m isobaths on the West Florida shelf (WFS) between Cedar Key and Naples (Steidinger et al., 1998; Walsh et al., 2009; Weisberg et al., 2009) in the eastern Gulf of Mexico (GOM). Subsequent physical transport within the

bottom Ekman layer (Weisberg et al., 2009) plays a critical role in the timing and location of the blooms relative to both nutrient sources and grazing stresses (Walsh et al., 2009, 2011a). Hence, the economic and health impact of local red tides to adjacent human population centers depends greatly upon both the availability of nutrients and herbivores during physical transport of the bloom.

Based upon recent data from 175 cruises on the WFS during March 1998–December 2001 (Walsh and Steidinger, 2004), we arrived at a consensus on a repetitive sequence of required events for annual red tide formation in the GOM (Walsh et al., 2006). Weak upwelling by the Loop Current at the shelf-break (Weisberg and He, 2003) provides Caribbean seed populations of the N₂ fixing cyanophyte, *Trichodesmium erythraeum*, within a nutrient milieu of low nitrogen/phosphorus (N/P) ratios on the WFS. Background *K. brevis* populations of ~0.01 µg chl l⁻¹ occur throughout the GOM (Geesey and Tester, 1993). The low N/P ratios of < 6 on the central WFS are

* Corresponding author. Tel.: +1 727 553 1112; fax: +1 727 553 1189.

E-mail addresses: lenes@marine.usf.edu (J.M. Lenés),

bdarrow@marine.usf.edu (B.P. Darrow), jwalsh@marine.usf.edu (J.J. Walsh),

jolliff@nrlssc.navy.mil (J.K. Jolliff), chen@marine.usf.edu (F.R. Chen),

weisberg@marine.usf.edu (R.H. Weisberg), lzheng@marine.usf.edu (L. Zheng).

the consequence of (1) estuarine supplies of leached Miocene phosphorite deposits, and (2) different rates of element recycling of plankton debris (Walsh et al., 2006).

Within the WFS, these phosphorus-rich nutrient supplies modulate seasonal phytoplankton succession after the initial diatom spring bloom, once summer deposition events of iron-laden Saharan dust allow *Trichodesmium* blooms to utilize ubiquitous dissolved dinitrogen gas (N_2) of otherwise nitrogen-poor seawater near the shelf-break (Lenés et al., 2001; Walsh and Steidinger, 2001). The ambient low stocks of nitrate (Masserini and Fanning, 2000) and selective grazing stresses exerted by copepods (Kleppel et al., 1996) place the diatoms at a competitive disadvantage here, compared to the slower growing diazotrophs and *K. brevis* (Walsh et al., 2001a, 2003, 2006). These co-occurring non-siliceous phytoplankton populations initially reside in the bottom Ekman layer due to similar diel vertical migration patterns, with the sun-adapted diazotrophs seeking higher phosphate and the shade-adapted dinoflagellates seeking lower light (Walsh et al., 2006). Fall upwelling events both resurface these phytoplankton residents of the bottom Ekman layer higher into the euphotic zone and transport them shoreward (Walsh et al., 2003; Weisberg and He, 2003; Weisberg et al., 2009), such that shelf-shading components of these toxic dinoflagellate populations can be finally detected by satellites.

In contrast, the faster-growing diatoms otherwise win the spring phytoplankton competition within GOM coastal waters (Gilbes et al., 1996; McPherson et al., 1996; Philips and Badylak, 1996; Dortch et al., 1997; Bledsoe and Philips, 2000; Gilbes et al., 2002; Qian et al., 2003; Jurado et al., 2007; Heil et al., 2007), where both dissolved nitrate, silicate, and iron stocks, as well as herbivores, are sometimes abundant in the estuaries, until seasonal silica-limitation ensues here and on most shelves (Walsh et al., 2011b). Farther offshore, the usual nitrate/silicate ratios do not favor diatom competitors on the WFS (Walsh et al., 2003). Moreover, both initial excretion and then lysis of the offshore *Trichodesmium* populations during their bloom decay can provide a unique nutrient source for red tides on the outer shelf (Walsh and Steidinger, 2001; Lenés et al., 2001, 2008; Mulholland et al., 2004, 2006; Walsh et al., 2006; Lenés and Heil, 2010), which the non-migratory diatoms evidently do not access.

These recycled nutrients in the form of dissolved organic nitrogen (DON), i.e., urea favored by *K. brevis* (Steidinger et al., 1998), and dissolved organic phosphorus (DOP), can be utilized by these toxic dinoflagellates (Vargo and Howard-Shamblott, 1990), giving them a competitive advantage over faster growing phytoplankton that prefer inorganic nutrient sources. Once seasonal *K. brevis* biomass has exceeded $\sim 1 \times 10^5$ cells l^{-1} , i.e., concentrations great enough to cause fish kills (Landsberg, 2002), high fish decomposition rates of up to 50% per day prevail within warm summer Florida waters (Stevenson and Childers, 2004), quickly converting particulate nutrients of fish flesh to the dissolved pools.

Walsh et al. (2006) estimated that there was ~ 1 individual fish per m^2 as photographed within the August 1947 drift lines of coincident dead fish, diazotrophs, and toxic dinoflagellates (Gunter et al., 1948). These fish populations were dominated by white grunts (*Haemulon plumieri*), pinfish (*Lagodon rhomboides*), and thread herring (*Opisthonema oglinum*). Previous estimates of mean fish wet weight (ww) of 90 g, dry weight (dw) of 25% ww, N content of $\sim 10\%$ dw, and P content of 0.7% dw suggested a potential nutrient supply for the maintenance of a red tide of $\sim 16 \mu\text{mol PN kg}^{-1}$ and $\sim 0.5 \mu\text{mol PP kg}^{-1}$ within a 10-m euphotic zone (Walsh et al., 2006).

In addition to decomposing cyanophytes and dead fishes, several other nutrient sources such as benthic flux (Darrow et al., 2003), ground water loading (Hu et al., 2006), riverine discharge (Brand and Compton, 2007), and zooplankton excretion

(Lester, 2005; Lester et al., 2008) may all contribute to the development and maintenance of *K. brevis* blooms. While the relative role of each nutrient source is still in question, it is clear that *K. brevis* is an opportunistic organism capable of utilizing all available resources (Vargo et al., 2008).

Therefore, continued development of validated simulation models of those environmental factors which lead to interannual successes and failures of “red tides” of *K. brevis* becomes increasingly important in eventual operational forecasts of their spatio-temporal bloom dynamics (Walsh et al., 2011c), by teasing out the relative role of each nutrient source in a heuristic mode. Of greater importance, however, will be eventual prudent management strategies for this and other pending future HABs of Florida waters (Walsh et al., 2011a).

Over the last 50 years, at least 15 simple (Slobodkin, 1953) and increasingly more complex (Walsh et al., 2001a, 2002, 2003; Jolliff, 2004; Milroy et al., 2008; Lenés et al., 2008) models of red tides in the eastern GOM have explored these earlier hypotheses, with some numerical formulations relying on synoptic estimates of satellite color signals for validation data (Jolliff et al., 2003; Walsh et al., 2006, 2009). We also used this remotely sensed surface information for initial and boundary conditions, providing constraints on which model parameters can reproduce both the seasonal succession of biochemically mediated dominant groups of phytoplankton and the complex ecological trophic cascade for initiation of more recent larger red tides of (1) *K. brevis* and (2) a competing, previously cryptic saxitoxic dinoflagellate *Pyrodinium bahamense* in the GOM (Walsh et al., 2006, 2011a).

People-killing HABs of the latter *P. bahamense* were involved in more than 100 deaths of humans, upon consumption of saxitoxin-adulterated sea food from the South China and eastern Caribbean Seas over the last few decades (Walsh et al., 2011a). Future simulation studies must thus address what are the “rules of engagement” for relatively benign ichthyotoxic *K. brevis* on the WFS to be replaced there and downstream by saxitoxic *P. bahamense*, whose poisons can be much more deadly to humans than sarin, curare, and brevetoxins.

Yet, the simpler objective of the present study was to evaluate the fidelity of an already complex, multi-species biochemical model for simulation of those ecological processes, which were required for the initiation and maintenance of *K. brevis* HABs on the WFS (Fig. 1). The model was thus quasi-independent of the three-dimensional (3-D) circulation and ignored any dinoflagellate competition between brevetoxic and saxitoxic poison sources. Therefore, we present the hindcasts for the 2001 red tide of *K. brevis*, utilizing the one-dimensional (1-D) form of the Harmful Algal Bloom SIMulations (HABSIM) model in the vertical dimension to test its fidelity with four different cases, calibrated against prior in situ cell counts and subject to a sensitivity analysis of the model's parameters. We then discuss needed additions to bring to fruition operational forecasts of WFS HABs.

Accordingly, even more complex future 3-D HAB forecasts would then involve revised ecological formulations of time-dependent selective nutrient regeneration, based on the present simulation analysis. But, to predict the outcome of competition of the relatively benign fish-killer *K. brevis* against the very poisonous *P. bahamense* to humans under nutrient-depleted conditions (Walsh et al., 2011a), spatial teleconnections of these two dinoflagellate HABs must also be explicitly considered within the shelf waters and estuaries of the GOM and the downstream South Atlantic Bight.

Future answers to complex questions about the possible impacts of legislated changes of fertilizer applications to lawns and agricultural crops unfortunately require complex, coupled biophysical models. Here, we evaluate the performance of HABSIM with 95 parameters, providing insight to the requirements of the

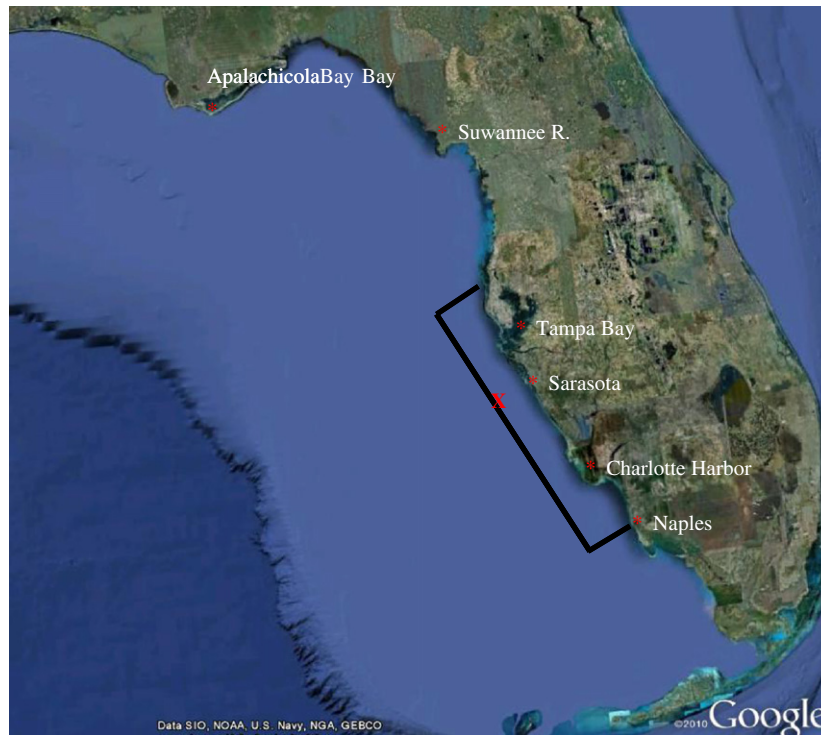


Fig. 1. Location of the one-dimensional model (X) west of Sarasota above the 20-m isobath in relation to Tampa Bay and Charlotte Harbor. The bounded area represents the region over which the maximum weekly *Karenia brevis* concentrations were obtained during 2001, for validation of the present model.

final generation of operational HAB models of the southeastern United States, within a forthcoming era of ecosystem-based management of marine biotic resources, now perturbed by overfishing, rising water temperatures, and oil spills.

2. Methods

The present HABSIM version consisted (Fig. 2) of 24 state variables: temperature, salinity, k_z for vertical mixing, spectral light, colored dissolved organic matter (CDOM), dissolved organic carbon (DOC), dissolved organic nitrogen (DON), dissolved organic phosphorus (DOP), dissolved inorganic carbon (DIC), nitrate + nitrite (NO_3), ammonium (NH_4), phosphate (PO_4), silicate (SiO_4), iron (Fe), four functional groups of phytoplankton (diatoms, microflagellates, *T. erythraeum*, and *K. brevis*), fecal pellets, ammonifying and nitrifying heterotrophic bacteria, detritus, larval fish, adult fish, and sediment microbiota.

The model had five submodels of (1) circulation, (2) dust deposition, (3) bio-optics, (4) pelagic ecological processes, and (5) benthic ecological processes, of which the last four compose HABSIM (Fig. 2). The last two were forced by outputs of the first three submodels. HABSIM was built upon the structure of previous ecological models (Walsh et al., 2001a,b, 2002, 2003, 2006; Jolliff et al., 2003; Jolliff, 2004; Lenés et al., 2008; Darrow, 2008; Milroy et al., 2008). Therefore, we limit the methods section to description of the major modifications and additions. A complete set of equations is presented in Section 6, Math formulae, while the model parameters are in Table 1.

2.1. Physical processes

The model had a 1-m vertical resolution over 20 depth levels of the water column, with one sediment layer of 1 cm thickness. A 30 s time step was used, beginning on 1 January 2001. The model was

spun-up for 3 months with simulation results shown from April–December 2001. It was positioned at the 20-m isobath (ECOHAB station 29 at $\sim 27.17^\circ\text{N}$, 82.90°W) southwest of Sarasota, FL (Fig. 1). Physical mixing of the model in the vertical direction, k_z , was calculated with a Mellor–Yamada Level 2.5 turbulence closure scheme (Mellor and Yamada, 1982), in which daily average wind speeds (Fig. 3(a)) were obtained from the National Data Buoy Center (NDBC) observations ~ 195 km WNW of Tampa, FL.

Daily temperature and salinity profiles (Fig. 3(b) and (c)) were calculated for the study site (Fig. 1) from the WFS circulation model (Barth et al., 2008; Weisberg et al., 2009), which is a regional application of ROMS (Regional Oceanic Modeling System, e.g., Shchepetkin and McWilliams, 2005) nested in HYCOM (HYbrid Coordinate Ocean Model, e.g., Chassignet et al., 2003). As such, it is fully 3-D and baroclinic, driven by complete physical forcing fields (deep-ocean fluxes across the open boundary from HYCOM and local momentum and buoyancy fluxes over the eastern GOM and WFS) with approximate 2–5 km horizontal resolution.

The internal light fields, as well as the water-leaving radiances, were computed from the bio-optical submodel's inherent optical properties. They were a function of some of the absorption and backscatter properties of seawater and the state variables of the ecological model, i.e., total phytoplankton biomass, total heterotrophic bacteria, CDOM, particulate detritus, and inorganic suspended sediments (Jolliff, 2004). Light at any given depth was determined using the Beer–Lambert law of exponential decay, with appropriate attenuation coefficients for blue and red light determined as a function of the concentrations/stocks of CDOM and equivalent chlorophyll biomass of the phytoplankton within the overlying water.

2.2. Biological processes

2.2.1. Phytoplankton competition

Debate over the feasibility of multi-plankton functional types (PFTs) and enhanced complexity, versus simpler model formulations,

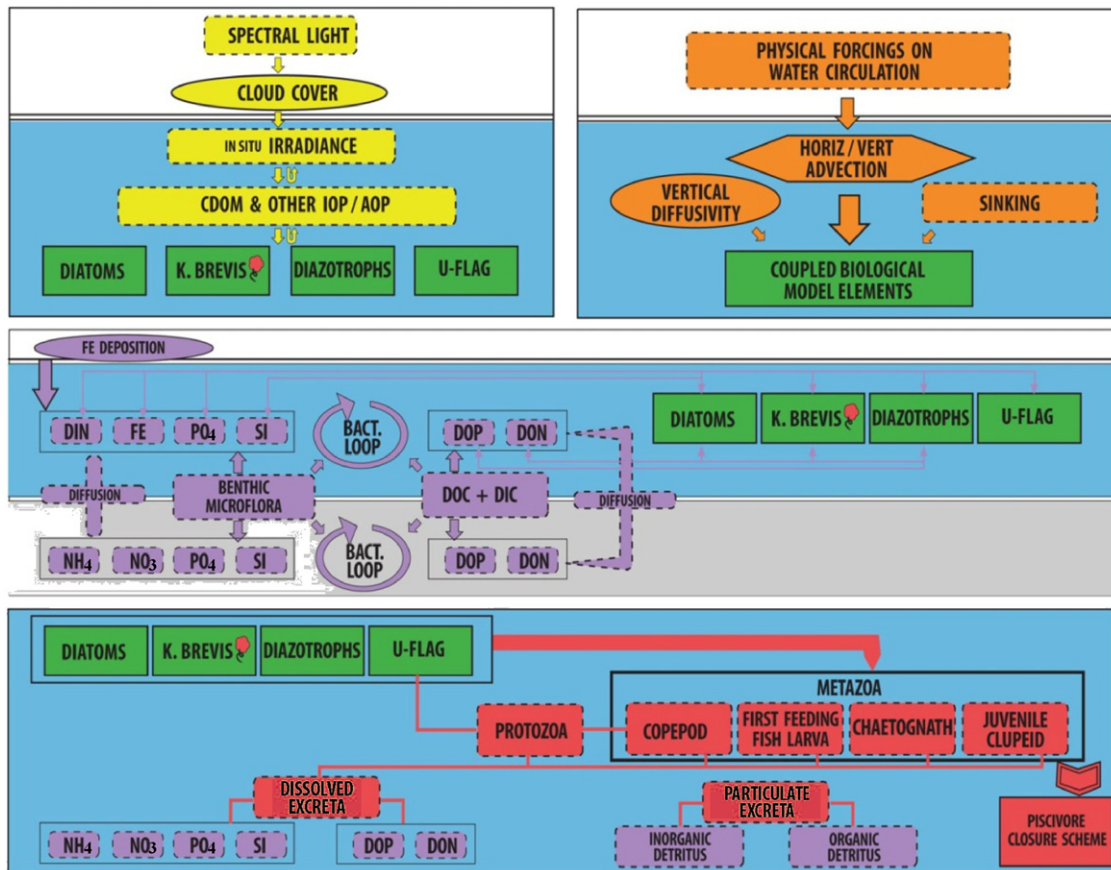


Fig. 2. Schematic of the HABSIM model with a color coded breakdown of the five components: green= pelagic phytoplankton; orange= physical model; yellow= optical model; purple= nutrient pathways; and red= loss to higher trophic levels. The blue area represents the water column and the gray area represents the benthos. (For interpretation of the references to color in this figure legend, the reader is referred to the web version of this article.)

continues to rage within the oceanographic community (Anderson, 2005; Flynn, 2005; Hood et al., 2006; Friedrichs et al., 2007, 2009). While all choices have trade-offs, it is critical that model variables and parameterizations are built upon the insights of simpler models (Thingstad et al., 2010). Given the inadequate results of a decade of such WFS models, we added a higher level of complexity in conjunction with the four PFTs to capture the annual planktonic succession and multiple trophic pathways that lead to the dominant HABs of toxic dinoflagellates on the WFS (Walsh et al., 2011a).

On most continental shelves, microflagellates follow the spring diatom bloom within a typical seasonal succession of phytoplankton, as functions of light availability, water column stability, nutrient resources, gravitational settling, and herbivore grazing demands. Furthermore, on the WFS, when episodic strong upwelling at a NO_3/PO_4 ratio of ~ 16 from the deep GOM prevails, nitrate-assimilating diatoms again dominate in both the “real world” and in models (Walsh et al., 2001a, 2001b, 2003).

Similarly, the usual spring succession of first diatoms can be fueled by nutrient supplies from northern estuaries in a N/P ratio > 16 (Walsh et al., 2006). For example, these siliceous phytoplankton win within March plumes of the northern Mississippi (Dortch and Whitley, 1992; Fahnenstiel et al., 1995), Apalachicola (Gilbes et al., 1996, 2002), Suwannee (Bledsoe and Philips, 2000) Rivers, and to less extent of the southern Peace (McPherson et al., 1996), and Shark (Jurado et al., 2007) Rivers until the summer rains begin, over near shore regions of the eastern GOM.

Zooplankton stocks respond on the WFS by maximal accumulation of biomass in May, following a spring peak of secondary production of WFS herbivores associated with low surface salinities, i.e., < 36.0 found above the 30-m isobath of the Florida

Middle Ground (FMG) in 1969–1970 at $\sim 28.50^\circ\text{N}$, 84.25°W (Austin and Jones, 1974). Another shelf-wide time series of zooplankton surveys during 1972–1974 subsequently found the same amount of spring maximal zooplankton biomass of ~ 250 ml displacement volume 1000 m^{-3} throughout the water column on the FMG, i.e., to the northwest of the study site (Fig. 1), during May 1970 and May 1973, 1974 (Austin and Jones, 1974; Houde and Chitty, 1976; as redrawn in Walsh et al., 2011c).

This FMG location is within the recurrent seasonal chlorophyll plumes of spring diatoms on the northern WFS, derived from local nutrient supplies of the Suwannee and Apalachicola Rivers, as observed during March 1992 (Gilbes et al., 1996) and on 3–27 March 2001. A few months later, however, an inverse north–south gradient is observed for the spring zooplankton standing stocks, with 50% more of the metazoan biomass found south, than north, of Tampa Bay during May 1973 and 1974 (Houde and Chitty, 1976). Such spatial spring differences in accumulation of planktonic predators and algal prey on the WFS reflect net population growth increments of these herbivores, as well as both settling and grazing losses of their upstream phytoplankton prey, over upstream time and space.

A north–south gradient of organic matter of plankton debris accumulated each year in the WFS surficial sediments, with as much as 1–2% dry weight organic carbon found near the FMG (Walsh and Dieterle, 1994). But, little organic matter of < 0.5 dry weight organic carbon was instead deposited in sediments of the central WFS, since diatom fallout used to be only a major component on the northern shelf (Darrow et al., 2003), as a consequence of local freshwater nutrient loadings (Gilbes et al., 1996, 2002), prevailing circulation patterns (Weisberg et al., 1984,

Table 1
The model variables and parameters.

	Description	Value	Units
P _{1,2,3,4}	Diatoms, Microflagellates, <i>Trichodesmium</i> , <i>K. brevis</i>		mmol C m ⁻³
B _{a,n}	Ammonifying bacteria, Nitrifying bacteria		mmol C m ⁻³
Fe _d	Dissolved Iron		mmol Fe m ⁻³
Fe _c	Colloidal Iron		mmol Fe m ⁻³
DIC	Dissolved Inorganic Carbon		mmol C m ⁻³
DOC	Dissolved Organic Carbon		mmol C m ⁻³
DON	Dissolved Organic Nitrogen		mmol N m ⁻³
DOP	Dissolved Organic Phosphorus		mmol P m ⁻³
NH ₄	Ammonium		mmol N m ⁻³
NO ₃	Nitrate		mmol N m ⁻³
PO ₄	Phosphate		mmol P m ⁻³
SiO ₄	Dissolved Silica		mmol Si m ⁻³
D	Detritus		mmol C m ⁻³
Z	Fecal Pellets		mmol C m ⁻³
F	Fish		mmol C m ⁻³
(C:N) _{1,2,3,4,a,n}	Nitrogen to Carbon ratio of phytoplankton and bacteria	6.63,6.63,6.6,6.3,5.5	
(C:P) _{1,2,3,4,a,n}	Phosphorus to Carbon ratio of phytoplankton and bacteria	106,106,122,106,53,53	
(C:Fe) _{1,2,3,4,a,n}	Iron to Carbon ratio of phytoplankton and bacteria (x10 ³)	15,25,2,20,15,15	
(C:Chl) _{1,2,3,4}	Carbon to chlorophyll ratio of phytoplankton	50,100,200,30	
T	Temperature		°C
Tr	Transport		m ² s ⁻¹
σ	Vertical coordinate		
w _{1,3,4}	Vertical migration/sinking rate for phytoplankton	0.5,0.0,*	m day ⁻¹
σ _{max3,4}	Maximum vertical migration rate for P ₃ , P ₄	77,23	m day ⁻¹
g _{1,2,3,4,a,n}	Growth rate of phytoplankton and bacteria		day ⁻¹
γ _{1,2,3,4}	Grazing rate on phytoplankton	0.02,0.06,0.02,0.01	day ⁻¹
ε _{1,2,3,4,n,a,f}	Fraction of growth respired	0.1,0.15,0.5,0.25,0.7,0.7,0.3	
ψ ₁	Fraction of diatom growth excreted	0.04	
l _{1,2,3,4}	Lysis rate of phytoplankton	0.008,0.2,*0.01	day ⁻¹
m _{a,n}	Mortality rate of ammonifying bacteria, nitrifying bacteria	0.086,0.086	day ⁻¹
β _{Fe,DON}	Photolysis rate of colloidal iron, DON	2.01,0.00017	mmol m ⁻³ day ⁻¹
α	Scavenging rate		mmol m ⁻³ day ⁻¹
K _{Fe}	Dissolved iron from atmospheric dust		
q _{1,2,3,4}	Fraction of lysed phytoplankton to detritus pool	0.1,0.1,0.1,0.1	
K _d	Decay rate of detritus	0.13	day ⁻¹
w _{D,Z}	Sinking rate of detritus, fecal pellets	0.1,100	m day ⁻¹
A _{1,2,3,4}	Fraction of grazed phytoplankton to fecal pellets	0.5,0.15,0,0.5	
b _{1,2,3,4}	Fraction of grazed phytoplankton to fish	0.075,0.045,0,0.075	
k _z	Fecal pellet decay rate	0.13	day ⁻¹
f	Fraction of grazed phytoplankton excreted by fish as fecal pellets	0.6	
k _{diss}	Dissolution rate of siliceous detritus/fecal pellets	0.6	day ⁻¹
o _{1,2,3,4}	Fraction of lysed material to DOM	0.9,0.9,0.9,0.9	
j _{1,2,3,4}	Fraction of grazed material to DOM	0.2,0.12,0.55,0.2	
k _{fd}	Decay rate of fish		day ⁻¹
k _h	coefficient of eddy diffusivity		m ² s ⁻¹
I _z	PAR at depth		
I _{sat1,2,3,4}	Light saturation intensity for each phytoplankton group	190,275,400,65	μE m ⁻² s ⁻¹
μ _{1,2,3,4,a,n}	Temperature specific maximum growth rate for phytoplankton	2.2,1.8,0.7,0.8,1.3,1.3	day ⁻¹
k _{nh4} - 1,2,4,n	half saturation constant for NH ₄	1.5,0.3,0.5,0.25	mmol m ⁻³
k _{no3} - 1,2,4	half saturation constant for NO ₃	1.0,0.3,3.0	mmol m ⁻³
k _{po4} - 1,2,3,4,n	half saturation constant for PO ₄	0.2,0.2,0.1,0.2,0.1	mmol m ⁻³
k _{si04} - 1	half saturation constant for SiO ₄	0.5	mmol m ⁻³
k _{DON} - 4,a	half saturation constant for DON	1.5,1.5	mmol m ⁻³
k _{DOP} - 3,4,a	half saturation constant for DOP	0.1,0.4,0.5	mmol m ⁻³
k _{Fed} - 1,2,3,4	half saturation constant for Dissolved Fe	5.5,500,5	10 ⁻⁶ mmol m ⁻³
α _{max}	maximum iron scavenging rate	0.62	day ⁻¹
k _z	iron scavenging coefficient	0.0015	
l _{tmax}	maximum <i>Trichodesmium</i> lysis rate	0.3	day ⁻¹
δ	fraction of maximum <i>Trichodesmium</i> growth due to nutrient limitation		

2009), and prior herbivore abundances (Houde and Chitty, 1976), even before long-term reductions of grazing stresses as part of a recent trophic cascade (Walsh et al., 2011a).

After sinking of the ungrazed parts of the estuarine-driven “regular” spring diatom bloom here (Hitchcock et al., 2000), sequestration of remineralized ammonium by benthic microflora instead triggered 6-fold seasonal increments of sediment chlorophyll (Darrow et al., 2003). Increases of the microflagellate stocks also occurred (Walsh et al., 2003) in response to the recycled nutrients, not captured by the phytobenthos. Since protozoans heavily grazed the microflagellates on the WFS

(Kleppel et al., 1996), the recycled nutrients were quickly transferred up the trophic ladder.

This removal process cleared the phytoplankton stage (Hutchinson, 1965) for summer fertilization of poorly grazed, slow growing diazotrophs and fall red tides in the low N/P waters of the WFS (Walsh et al., 2003, 2009). To simulate the consequences of the spring nutrient supply from the northern GOM rivers, a nutrient pulse of 1.0 μmol NO₃ kg⁻¹, 0.1 μmol PO₄ kg⁻¹, and 2.0 μmol SiO₄ kg⁻¹ was added to the upper 10-m of the model’s 20-m water column on 16 March 2001 of the baseline case of the model.

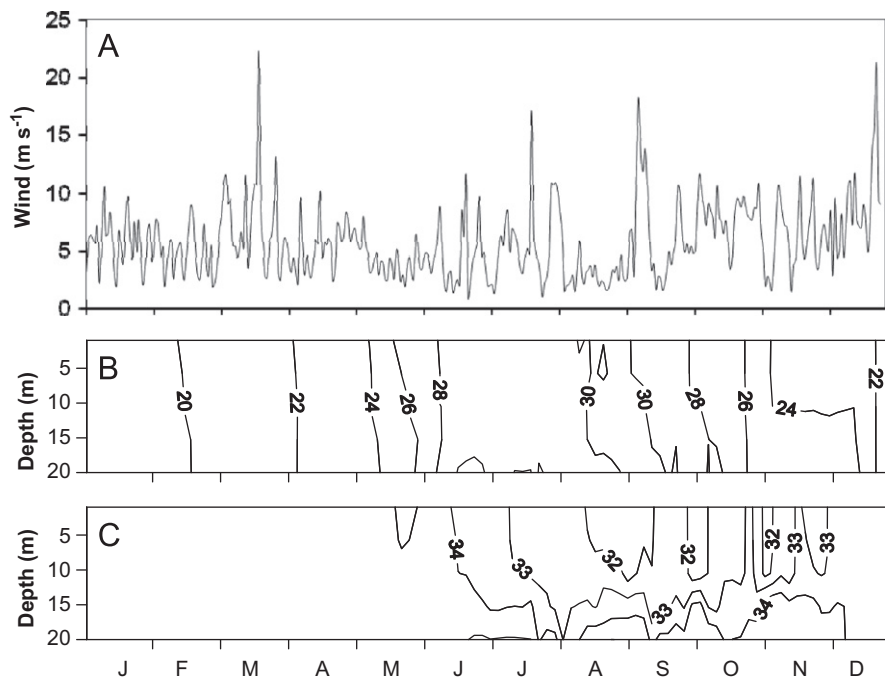


Fig. 3. The 2001 mean daily (A) wind speed (m s^{-1}) at the National Data Buoy Center (NDBC) at station 42036, 195 km WNW of Tampa, FL, as well as the (B) temperature ($^{\circ}\text{C}$) and (C) salinity fields calculated from the WFS ROMS circulation model versus depth (Barth et al., 2008).

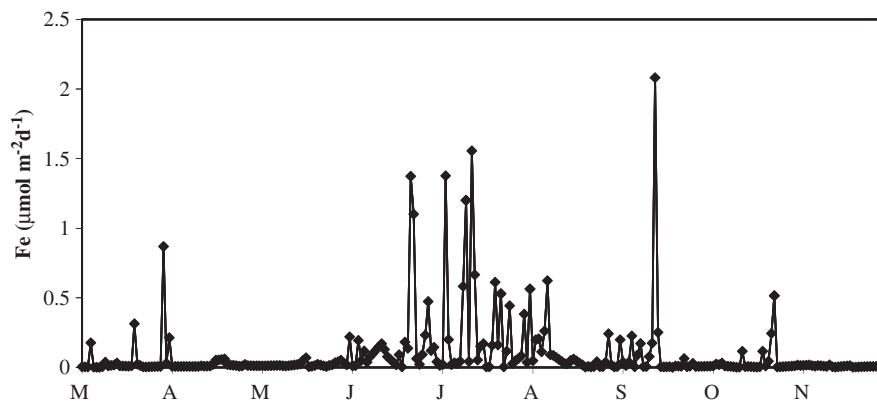


Fig. 4. The 2001 daily influx of total dissolved iron ($\mu\text{mol m}^{-2} \text{day}^{-1}$) to the West Florida shelf surface waters as a perturbation condition. Atmospheric dust concentrations at Miami and daily rainfall at Tampa International Airport were used to calculate both wet and dry deposition (after Lenés et al., 2008).

2.2.2. Element stoichiometry

To initiate nitrogen-fixation, iron of Saharan dust origin was injected at the surface of the model in this first case during mainly June–July 2001 (Fig. 4). In each case of the model (with and without estuarine, diazotroph, and dead fish sources of nutrients), phytoplankton competition among the PFTs was effected by variations in rate parameters, such as: the temperature-dependent maximal growth; photosynthesis at saturation light intensity; half-saturation constants for uptake of nutrients; respiration; excretion; grazing; settling; and migration for each group of phytoplankton and benthic microalgae (Table 1).

In this complex ecological model, the carbon-based growth rates of pelagic and benthic diatoms required nitrate and silicate in a constant molar ratio of 100 C/16 N/16 Si/1 P (Table 1) for balanced growth. The other PFTs had the same N/P Redfield molar body ratios of 16/1 (Table 1), such that the model's phytoplankton decomposition and recycling through the bacterial pool occurred at this ratio of 10/1, not that of selective remineralization of phosphorus (Grill and Richards, 1964; Kamatani, 1969). These

bacterial recycling processes instead yielded an initial dissolved N/P ratio of ~ 4 , observed in benthic depocenters of shallow waters, downstream of river-grown diatoms on the northern GOM (Walsh et al., 2006).

Neglect of this separate time-dependence of element recycling of phytoplankton debris in the model led eventually to phosphorus-limitation and thus unrealistic time lags of the simulated *Trichodesmium* and subsequent *Karenia* blooms. While presently of heuristic interest, such a failure in an operational model would falsely predict both late arrivals of *K. brevis* HABs on the beaches and inadequate warnings of associated fish kills and asthma attacks.

The assumed C/chl weight ratios of 30–50 for diatoms, instead of ~ 200 found for all particulate matter during the NEGOM and ECOHAB cruises (Jochens and Nowlin, 1999; Heil et al., 2004), yielded a particulate PN/chl ratio ($\mu\text{mol}/\mu\text{g}$) of ~ 0.6 for siliceous phytoplankton, as measured during other diatom blooms (Walsh et al., 1978). Finally, a composite chlorophyll content of $\sim 0.5 \times 10^{-6} \mu\text{g cell}^{-1}$ implied a mixed diatom population of 90%

small (8 μm) and 10% large (50 μm) forms of these netplankton (Walsh et al., 2001a), with a maximal growth rate of $\sim 2.2 \text{ day}^{-1}$ at 30 °C (Table 1). They had an intermediate light saturation intensity of 190 $\mu\text{mol photons m}^{-2} \text{ s}^{-1}$.

The second functional group of the model was small microflagellates of 6–8 μm diameters, with a C/chl ratio of ~ 100 , and a chlorophyll content of $\sim 0.5 \times 10^{-6} \mu\text{g cell}^{-1}$ (Table 1). They had a similar maximal growth rate of the diatoms, i.e., ~ 1.8 per day at 30 °C, but a light saturation intensity of 275 $\mu\text{mol photons m}^{-2} \text{ s}^{-1}$, reflecting their sun-adaptation as neutrally buoyant particles at the sea surface. In addition, both of these functional groups utilized only inorganic forms of N and P. Therefore, selective grazing losses determined the outcome of the competition between these two fast-growing groups in the model, unless Si-limitation prevailed.

2.2.3. Herbivory

When diatoms were present, copepods actively selected this food item in the model, as observed on the WFS (Kleppel et al., 1996). Instead, the mean grazing loss of the smaller microflagellates to protozoan micro-zooplankton in the GOM was $\sim 82\%$ of their realized growth rate (Fahnenstiel et al., 1995), while the larger diatoms suffered minimal predation by ciliates (Strom and Strom, 1996). Therefore, we imposed grazing stresses on first the diatoms and microflagellates, with minimal losses to *K. brevis* (Turner and Tester, 1997) and *Trichodesmium* (O'Neil and Roman, 1992; Guo and Tester, 1994). If the daily food demand of the copepods was not met by diatoms, they then consumed protozoans in the model (Walsh et al., 2001b). In turn, microflagellate losses to protozoans were a function of just the algal prey biomass (Table 1), since the unicellular herbivores were an implicit state variable of the model.

Accordingly, the model's total phytoplankton community was grazed by both copepods and protozoans, which were eaten in turn by competing chaetognath rivals of the larval clupeids (Fig. 2). These primary carnivores thus consumed herbivorous zooplankton and were the prey of higher trophic levels (Fig. 2). Although copepods generally shun *K. brevis* (Tester et al., 2000), the dominant smaller WFS calanoid copepods, e.g., *Paracalanus quasimodo*, would eat this species if other prey were not available within downstream North Carolina shelf waters (Turner and Tester, 1997).

We also found cells of *K. brevis* in the mouths of *Temora turbinada* and *Centropages velificatus* on the WFS (Walsh et al., 2003), such that the model's grazing coefficient was 0.01 on *K. brevis* (Table 1), compared to 0.70 on diatoms (Walsh et al., 2003). However, the copepods ate mainly diatoms (Kleppel et al., 1996) as they were the dominant phytoplankton community on the WFS in early spring of the "real world" (Gilbes et al., 1996, 2002) and the model.

2.2.4. Autotrophic processes

In contrast, *K. brevis* had a maximal growth rate of only $\sim 0.8 \text{ day}^{-1}$ (Walsh et al., 2001a) at 30 °C in our model, with a larger cellular chlorophyll content of $\sim 5.0 \times 10^{-6} \mu\text{g chl cell}^{-1}$ and a light saturation intensity of 65 $\mu\text{mol photons m}^{-2} \text{ s}^{-1}$ (Table 1), reflecting their shade-adaptation (Walsh et al., 2002). *K. brevis* can utilize urea, vitamins, amino acids, and other forms of organic nitrogen at varying rates (Baden and Mende, 1979; Shimizu and Wrensford, 1993), providing a possible niche for these and other dinoflagellates (Dennison and Abal, 1999; Glibert and Terlizzi, 1999). Although the half-saturation constant for NH_4 uptake by *K. brevis* was lower than that for urea and nitrate (Table 1), uptake of all three nitrogen pools (labile DON, NH_4 , and NO_3) occurred in the model.

The toxic dinoflagellates swam vertically at a speed of 1 m h^{-1} , in response to a light cue (Walsh et al., 2002; Kerfoot et al., 2004). The diatoms aggregated, settling as a function of their biomass (Walsh and Dieterle, 1994), and the microflagellates did not sink. The diazotrophs also vertically migrate in relation to the light field by controlling their buoyancy (Walsby, 1978, 1992; Villareal and Carpenter, 1990). Thus, vertical ascents and descents of *Trichodesmium* in the model occurred at a speed of $\sim 3.2 \text{ m h}^{-1}$ (Lenés et al., 2008).

Finally, *Trichodesmium* had a similarly slow maximal growth rate of $\sim 0.7 \text{ day}^{-1}$ at 30 °C as *K. brevis* (Lenés et al., 2005, 2008). However, the nitrogen-fixers were assigned a light saturation intensity (I_{sat}) of 400 $\mu\text{mol photons m}^{-2} \text{ s}^{-1}$ (Rueter et al., 1990, 1992) in the model, reflecting their light-adaptation (Lenés et al., 2005). Since the ambient dissolved nitrogen gas, N_2 , does not limit growth of these diazotrophs on the WFS, the realized gross growth rate for *Trichodesmium*, μ_3 , was determined by the least available resource of light or nutrients (Lenés et al., 2008), where dFe was dissolved iron:

$$\mu_3 = \mu^T \min \left[\frac{I_z}{I_{\text{sat}} e^{1-I_z/I_{\text{sat}}}}, \max \left(\frac{PO_4}{(k_{PO_4} + PO_4)}, \frac{DOP}{(k_{DOP} + DOP)} \right), \frac{dFe}{(k_{dFe} + dFe)} \right] \quad (1)$$

In eq. (1), μ^T was the maximum gross growth rate, adjusted for temperature-stress, T , from the measured temperature profiles, assuming that the *Trichodesmium* growth rate was maximal at temperatures > 20 °C (Carpenter, 1983). The Michaelis–Menten half-saturation constants for uptake of phosphate (k_{PO_4}), dissolved organic phosphorus (k_{DOP}), and iron (k_{dFe}) were specific to *Trichodesmium*. Phosphorus availability was calculated as TDP, where preferential uptake was given to PO_4 over DOP by imposition of a smaller half-saturation constant (Table 1).

High levels of alkaline phosphatase activity have been measured in phosphate-depleted diazotroph colonies (Yentsch et al., 1972; Stihl et al., 2001), indicating that *Trichodesmium*, like *Karenia*, can assimilate DOP (Vargo and Howard-Shamblott, 1990). Each PFT was thus assigned a unique mean C:N:Si:P:Fe molar ratio to accentuate their competition (Table 1). In conjunction with different half-saturation constants, the ability of each PFT to utilize different nutrient pools, and element-specific remineralization rates, helped compensate for the mathematical restrictions associated with the selection of the Monod limitation equations and fixed species-specific nutrient ratios.

We computed the 2001 daily influx of iron to WFS surface waters as perturbation conditions (Fig. 4). Measured atmospheric dust concentrations by Joe Prospero at Miami and daily rainfall at Tampa International Airport were used to calculate both wet and dry deposition (Lenés et al., 2008). The cellular N/Fe molar ratio of *Trichodesmium* (Table 1) was 1500 (Sanudo-Wilhelmy et al., 2001). Diatoms required 10-fold less dFe during synthesis of nitrate reductase for nitrate assimilation in the model, compared to what the diazotrophs needed in formation of nitrogenase during nitrogen fixation. Therefore, dFe inputs (Fig. 4) mainly influenced the growth of diazotrophs, via Eq. (1), due to their high Fe demand.

Trichodesmium populations of the model were minimally grazed, but they did undergo cell lysis as a function of nutrient limitation (Lenés et al., 2005, 2008), to mimic programmed cell death in response to nutrient stress (Berman-Frank et al., 2004, 2007). Photo-inhibition of *Trichodesmium* was ignored in HABSIM, because high saturation light intensities (Carpenter and Roenneberg, 1995) allow them to thrive within surface summer waters of the WFS (Lenés and Heil, 2010), while Subramanian et al. (1999) has shown that *Trichodesmium* both releases excess light energy as fluorescence and possesses high levels of photo-protective pigments.

2.2.5. Bacteria

Bacterial secondary production can be an order of magnitude higher within a red tide on the WFS than in surrounding waters (Heil et al., 2004). Thus, heterotrophs may be competing against *K. brevis* for utilization of the DON (Mulholland et al., 2004, 2006). Since bacteria also compete against the phytoplankton for both phosphate and ammonium in the GOM (Pakulski et al., 2000), they were included as explicit state variables (Table 1). The two distinct functional groups of the model were ammonifying and nitrifying bacteria (Darrow et al., 2003; Lenés et al., 2008). Like the autotrophic rates of the phytoplankton, the heterotrophic processes of the bacteria were impacted by the temperature fields (Kirchman, 2000; Ducklow, 2000). Their temperature-regulated net growth rate was a minimal function of the available nitrogen or phosphorus, in both organic and inorganic forms (del Giorgio and Cole, 2000). Specifically, ammonifiers assimilated the organic nutrient pools while the nitrifiers utilized the inorganic ones, but in N/P ratios of 10 in the model, not 4 of the “real world”. Bacteria had no simulated settling velocities in the model, because of their small size.

On the WFS, dissolved organic matter (DOM) tends towards low phosphorus content, with a large molar C/P ratio of 250 (Walsh et al., 2006). Instead, bacteria have a smaller molar C/P ratio of 53. The net result of these calculations in our model was that the bacteria competed with the phytoplankton for phosphate, when labile DOC was abundant. This result was consistent with the observations that DOC-rich aquatic systems tend towards P-limitation (Kirchman, 1994). Inclusion of two bacterial pools allowed for a differential response in nutrient remineralization dependent upon the nutrient concentrations within available pools.

2.2.6. Dead fish

Adult and juvenile fishes range over the WFS, harvesting local zooplankton food supplies, derived in turn from copepod herbivores eating diatoms and from copepod omnivores eating protozoans after their ingestion of microflagellates (Houde and Chitty, 1976; Kleppel et al., 1996). Diazotrophs (Guo and Tester, 1994) and *K. brevis* (Turner and Tester, 1997) are instead not readily consumed by zooplankton, nor indirectly by teleosts. Indeed, *K. brevis* may harvest the fish within an ecological role reversal of direct brevetoxic poisonings (Walsh et al., 2006; 2009). As with surface aggregations of diazotrophs, positively buoyant dead fish float and accumulate at frontal boundaries of the sea surface (Gunter et al., 1948). Such dead fish are thus a concentrated source of recycled nutrients within the euphotic zone, but derived from a larger area than that of the local water column.

These fish supplies of nutrients may be equivalent to those derived from dying *Trichodesmium* at the beginning of a red tide within offshore waters (Lenés and Heil, 2010). Thus, we have now included within the HABSIM model (Fig. 2) a positive feedback of the recycled organic nutrients (DON and DOP) from decaying fish, killed by *K. brevis*. Note that dissolved silicon was not replenished during this simulated remineralization process of nitrogen and phosphorus.

Yet, zooplankton biomasses of herbivores and omnivores were not explicit state variables of the model. Ingestion demands of two fish life history stages, or size classes, were instead used to compute the cumulative equivalent nutrient stocks of their zooplankton prey, ZP, i.e., ZP_{1,2} of Eq. (2) and Table 1.

$$\frac{\partial ZP_1}{\partial t} = -\frac{\partial w_z ZP_1}{\partial \sigma} + 0.60[a(1-\varepsilon_d)(\gamma_d P_d) + (1-\varepsilon_k)(\gamma_k P_k)] \cdot [1-0.30-0-0.01] \quad (2)$$

The first pool, ZP₁, represented food eaten by younger zoophagous fishes, while raised from copepods, grown in turn

on diatom and protozoan prey. We assumed that most of these zooplanktivore juvenile and larval fish would be young-of-the-year clupeids, undergoing larval recruitment of the dominant spring spawners (Houde et al., 1979), i.e., the thread herring (*O. oglinum*) and the scaled sardine (*Harengula jaguana*).

The second group of fish food, ZP₂, represented a background pool of cumulative prey eaten by older spawning adult fishes, and released when these fishes were poisoned. The adult fish pool was set as a homogeneous nutrient field (Table 1), provided from mortality of dead fish during toxic events. Therefore, ZP₂ was set to 5.0 μmol PN kg⁻¹ of fish body nitrogen, sampled during October 2001 on the WFS as the equivalent amount of recycled ammonium stocks found adjacent to dead fish.

To specify, when and where in the model, these life history stages of fishes were poisoned by toxic levels of *K. brevis*, an IF statement was employed. When the concurrent accumulation of *K. brevis* reached toxic levels (Landsberg, 2002), the cumulative supply of the zooplankton prey assimilated by clupeoids, ZP = ZP₁ + ZP₂, were released as DOM at that grid point. The rate of nutrient release was set at a maximal 50% of ZP per day, reflecting the highest dissolution rate of dead fish in warm Florida waters (Stevenson and Childers, 2004).

Sloppy feeding by copepods of this simple food chain leading to younger clupeoids was set to 50% (Walsh et al., 2003), such that half of the grazed phytoplankton became a DOM source within eq. (2) of the model. Accordingly, the cumulative ZP₁ food required by early life history stages of the clupeoids over the study site (Fig. 1) was estimated from other terms of Eq. (2). Of these, the first one of the settling velocity (w_z) was set to zero, in relation to the vertical coordinate system (σ). The smaller dead fish were also assumed to float at the surface, like the adults, as a consequence of internal gases released during decomposition.

In the second term of Eq. (2), 0.60 was the assimilation efficiency of copepod herbivores, feeding poorly on just diatoms, defined by the sloppy grazing coefficient, a , the specific grazing rate, γ_d , and a respiration rate of ε_d (Walsh et al., 2003). When the copepods ate protozoans, the efficiency of 0.60 was replaced by one of 0.80, reflecting higher quality food. The diatoms were a more palatable food source than *K. brevis*, which were ingested at a much smaller rate, γ_k , with a respiration rate of ε_k (Walsh et al., 2003). The daily loss components of the fish size class were calculated in the last term of Eq. (2). Respiration loss was 30%, while reproduction costs to the larval and juvenile fish were 0%, and removal by fish piscivores (groupers, mackerels, snappers) and humans was 1%.

2.2.7. Benthos

On the sea floor, any toxic dinoflagellates would have competitors in the form of both near-bottom diatoms and benthic microflora (Fig. 2). From prior measurements, the chlorophyll biomass of photosynthetic organisms within the upper one centimeter of WFS sediments was greater than that of the overlying water column. These phytobenthos were likely to intercept any ground water supplies of nutrients (Hu et al., 2006). However, upon recycling of their body N and P by bacteria, like pelagic diatom sources (Grill and Richards, 1964; Darrow et al., 2003), they represent another source of low N/P nutrients for utilization by the diazotrophs and red tides on the WFS. Accordingly, the sediment microflora were an additional state variable of the model (Fig. 2) in all four cases.

We assumed that the benthic microflora were diatoms (Darrow et al., 2003), with a maximum growth rate of ~0.5 day⁻¹ at near-bottom temperatures of 10 °C. Like *K. brevis*, they were also shade-adapted, with again a light saturation intensity of 65 μmol photons m⁻² s⁻¹ (Table 1; Darrow, 2008). However, unlike

Trichodesmium and the heterotrophic bacteria of the model, the benthic microflora only used inorganic forms of the nutrients (PO_4 , NH_4 , NO_3 , and SiO_4) with appropriate values of their half-saturation constants drawn from the literature (Darrow et al., 2003). Based upon temporal changes of microfloral biomass between April and July on the WFS, as well as between April and June on the Georgia shelf (Nelson et al., 1999), a grazing loss to the meiobenthos was imposed on the benthic diatoms of the model, similar to that of the pelagic diatoms from copepods. In the thin, well oxygenated sediment layer of the model, we ignored denitrification. The two benthic bacterial functional groups were identical to those in the water column.

2.3. Simulation cases

Four cases of the model were run to test the relative role of each major nutrient source during 2001. The baseline of Case 1 included three nutrient sources: discharge from the northern rivers; *Trichodesmium*; and dead fish. In each of the three subsequent cases, one source was deleted to quantify the impact on the simulated population levels of *K. brevis*, compared to field observations during 2001. Case 2 had no river pulse, while Case 3 had no *Trichodesmium* populations, and Case 4 had no fish kills. In terms of statistical goodness-of-fits of the model cases with observed cell counts of *K. brevis*, the simulated and observed chronologies were compared over two time periods: 1 April–31 December 2001 and 1 April–5 October 2001. The latter results are designated as Cases 1a, 2a, 3a, and 4a.

2.4. Validation data

In this study, we utilized monthly data collected during three cross-shelf sections off Tampa Bay, Sarasota, and Charlotte Harbor and two along shore transects from 1998–2002 (Fig. 1) as part of the NOAA/EPA ECOHAB: Florida and ONR HyCODE studies (Walsh and Kirkpatrick, 2008), with emphasis here on the 2001 observations. Hydrographic data and water samples were collected at 63 locations, with a Seabird CTD mounted on a rosette sampler of Niskin bottles. Species-specific phytoplankton cell counts were performed through microscopic examination, both during the cruises and along the shoreline. Vargo et al. (2008) have described the methodology used to determine some of the inorganic (NO_3 , PO_4 , SiO_4) and total dissolved nutrients (TDN, TDP), as well as the chlorophyll stocks.

Winter values were estimated from these data sources and linearly interpolated to initialize the model (Table 2). The seasonal mean distributions of the inorganic nutrients were compiled, when available at the 10-m and 25-m isobaths. However, contamination of the 2001 ammonium samples prevented back

calculation of DON by subtracting nitrate, nitrite and ammonium from TDN. Therefore, DON observations were not available for comparison with model hindcasts during the 2001 simulations. We instead used measurements of TDN ($\text{TDN} = \text{NO}_3 + \text{NH}_4 + \text{DON}$) and TDP ($\text{TDP} = \text{PO}_4 + \text{DOP}$) for nutrient validation of the model's fidelity. Finally, sensitivity simulations were run both to derive initial values for state variables that lacked in situ measurements and to evaluate the validity of the model's solutions.

In terms of biomass predictions of the different cases of the model, validation data of *K. brevis* cell counts during 2001 were obtained from the Florida HAB historical database maintained by the Florida Wildlife Commission's Fish and Wildlife Research Institute (FWC FWRI). Coastal circulation dramatically affects horizontal position of *K. brevis* blooms on the WFS (Weisberg et al., 2009; Walsh et al., 2009). In addition, most of the *K. brevis* data was collected in "an event response mode", precluding a consistent temporal time series at any one location.

However, maximal concentrations of phytoplankton, detected either at the sea surface by satellites (Walsh et al., 2011a), or at depth by in situ sampling of cell counts, all reflect a net "patchy" realization of the local population balances of the growth processes of photosynthesis and nutrient uptake, in relation to the loss processes of catabolism, sinking, and grazing. If one of these factors is altered significantly, i.e., either addition of nutrients, or reduction of grazing pressure, the next set of values of temporal-spatial maxima will accordingly reflect the new balances of population gains and losses within a local region of the WFS (Fig. 1).

Accordingly, our 1-day vertical model at a fixed position (Fig. 1) represented a cumulative WFS catchment basin of onshore and alongshore advection of phytoplankton populations during net biological growth and loss processes (Walsh et al., 2003). Thus, the weekly maximum *K. brevis* cellular concentrations were extracted from the FWC FWRI database, over both the surface (< 3 m) and bottom (within 5 m of bottom) within 35 km of the West Florida coast between Cedar Key and Naples (Fig. 1), for evaluation of the sensitivity cases of the model.

Such an approach allowed us to compare the simulated biochemical bloom dynamics independent of the horizontal physical processes and sampling bias, since this region (Fig. 1) comprised > 80% of the *K. brevis* samples (Young and Christman, 2006; Heil and Steidinger, 2008). These maximal *K. brevis* cell counts were converted to mmol C m^{-3} for comparison to the model output, using $5.0 \times 10^{-6} \mu\text{g chl cell}^{-1}$ and a C:chl ratio of 30 (Table 1). Given the prior concurrence of weekly mean cell counts of the *K. brevis*, when present and dominant along the West Florida coast, with satellite estimates of the total phytoplankton community (Walsh et al., 2011a), we feel that these additional observations of the time history of the red tides during

Table 2
Validation statistics and metrics applied to the *Karenia brevis* functional group by case. Statistics for cases 1–4 are calculated based on the full temporal model simulations. Statistics for cases 1a, 2a, 3a and 4a are through 5 October. Bold values indicate the "best fit".

Statistic	Case 1	Case 1a	Case 2	Case 2a	Case 3	Case 3a	Case 4	Case 4a
AE	44.254	5.475	34.760	−19.644	−37.838	−57.490	−36.043	−54.150
AAE	57.949	24.120	61.635	27.712	37.880	57.586	37.297	56.575
RMSE	92.525	42.655	98.329	54.252	84.915	99.904	83.872	98.091
RMSE/ \bar{P}	2.379	0.729	2.528	0.927	2.183	1.707	2.156	1.676
MEF	−0.462	0.747	−0.651	0.590	−0.231	−0.390	−0.201	−0.340
r^2	0.281	0.745	0.140	0.631	0.274	0.634	0.194	0.151

Average error (bias): $\text{AE} = (\sum(P_i - O_i))/n$; average absolute error: $\text{AAE} = (\sum|P_i - O_i|)/n$; root mean squared error: $\text{RMSE} = ((\sum(P_i - O_i)^2)/n)^{0.5}$; general standard deviation: RMSE/\bar{P} , where $\bar{P} = (\sum P_i)/n$; modeling efficiency: $\text{MEF} = (\sum(O_i - \bar{O})^2 - \sum(P_i - O_i)^2)/\sum(O_i - \bar{O})^2$; coefficient of determination: $r^2 = [\sum(O_i - \bar{O}) \cdot (P_i - \bar{P})]/(\sum(O_i - \bar{O})^2 \cdot \sum(P_i - \bar{P})^2)^{0.5}$, where n = the number of observations, O_i = the i th of n observations, P_i = the i th of n predictions, \bar{O} and \bar{P} are the observation and prediction averages (statistical equations after Biber et al., 2004; Stow et al., 2009).

July–December 2001 allow ease of interpretation of the results of the four case studies, from this admittedly complex model of Florida red tides of *K. brevis*.

2.5. Sensitivity analyses

Testing the reliability of an ecological model requires assessment of the input parameters. A sensitivity analysis of these ecological parameters also provides description of the needs for model improvement, indicating which state variables have the greatest impact on the ability of the model to replicate observations. In this model, we tested the sensitivity of 95 parameters in relation to the computed values of *K. brevis*, in statistical comparisons with the observations. The sensitivity of each model parameter was calculated (Franks et al., 1986; Fasham et al., 1990; Ji et al., 2006) by Eq. (3), in which $\Delta\text{Parameter}$ was the amount of variation of a 1% departure from the baseline value.

$$\hat{S} = \left| \frac{\Delta F / F}{\Delta \text{Parameter} / \text{Parameter}} \right| \quad (3)$$

In Eq. (3), \hat{S} was the index of sensitivity and ΔF was the change in concentration of *K. brevis*, compared to its value in the baseline simulation, F , caused by fluctuation of the specified model parameter. The prior studies defined a parameter to be sensitive, if $\hat{S} \geq 0.5$. The sensitivities of the simulated *K. brevis* blooms to some of the model parameters are shown in Fig. 5. Only the parameters with an index of > 0.1 are considered here (19 out of 95 parameters). We shall find that of the model's 95 parameters, only three were considered significantly sensitive: *K. brevis* grazing (γ_4); the molar phosphorus to carbon ratio of *K. brevis* ((C:P)₄); and the maximum growth rate of *Trichodesmium* (μ_3).

Six different statistical criteria (Table 2) were evaluated for each of the four separate cases to assess the predictive ability and efficiency of this version of the HABSIM model. The model results were compared against weekly surface and near-bottom maximal cell counts, when available, yielding estimates of: average error (AE); average absolute error (AAE); root mean squared error (RMSE); general standard deviation (RMSE/ \bar{P}); modeling efficiency (MEF); and the coefficient of determination, i.e., the square of the correlation coefficient (r^2). We utilized this set of quantitative metrics for univariate comparison of model results with observations as outlined by Biber et al. (2004) and Stow et al. (2009): average error (AE), average absolute error (AAE), root mean squared error (RMSE), general standard deviation (RMSE/ \bar{P}), modeling efficiency (MEF) and correlation coefficient (r^2). The coefficient of determination measures the tendency of the predicted and observed values to vary together, with an ideal value of 1. The root mean square error, average error, average absolute error, and general standard deviation all calculate the size of the difference between predicted and observed values, where values near zero indicate a close match. The modeling efficiency represents how well a model predicts relative to the average of the observations, where values near one indicate a close match between observations and predictions and a value less than zero indicates the observation average is a better predictor than the model results. The equations for each metric were listed in Table 2 and a more comprehensive description of the use of these metrics is available in Stow et al. (2009).

3. Results

3.1. Phytoplankton

The phytoplankton community of the model's baseline case reproduced initiation of the spring transition of microalgae, with

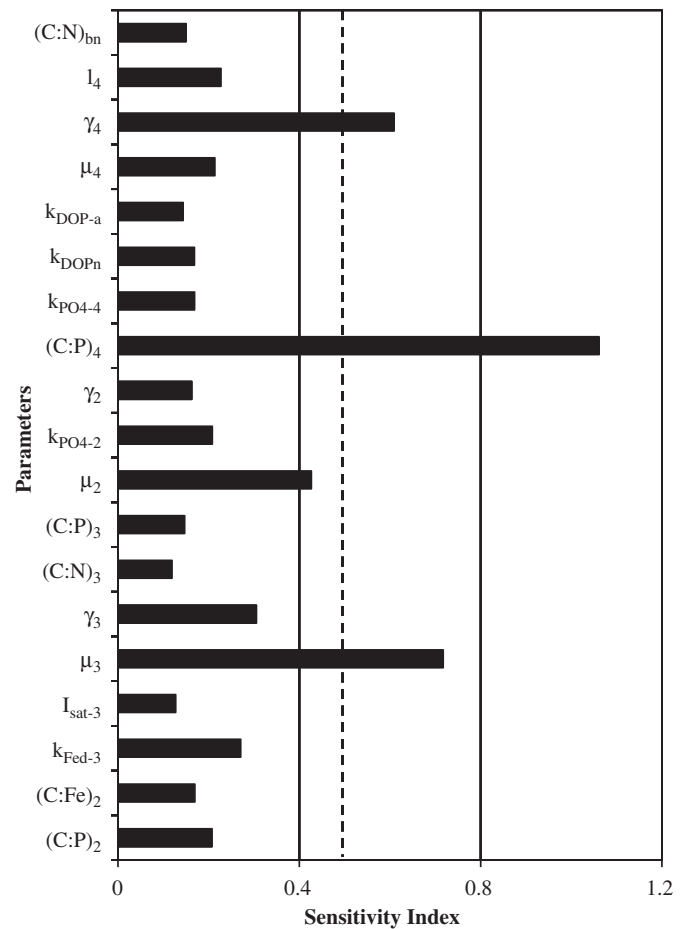


Fig. 5. Sensitivity of the 95 model parameters, of which only those parameters with a sensitivity of > 0.1 are shown.

a diatom pulse by 10 April of $> 1 \mu\text{mol C kg}^{-1}$ throughout the water column (Fig. 6(a)). These fast growing siliceous phytoplankton outcompeted the other phytoplankton for the inorganic nutrients injected at the surface on 16 March. The simulated injection of nitrate represented the annual pulse of nutrients from the northeastern GOM estuaries (Gilbes et al., 1996, 2002), with subsequent surface chlorophyll plumes. The modeled response was a ~ 2 week delay, relative to the observed chlorophyll feature on the northern WFS.

Such a time delay was consistent with an estimated transit time from the nutrient source region to the model site. The simulated diatoms were quickly removed from the model's water column by grazing and sinking, leading to a near bottom accumulation of $> 1 \mu\text{mol C kg}^{-1}$ during April (Fig. 6(a)). Note that the prior surface phytoplankton stocks of $> 1 \mu\text{g chl l}^{-1}$ observed during the 3–5 March 2001 ECOHAB cruise had also sunk out of the water column near the model's location by the 3–6 April cruise (Fig. 7).

When pelagic diatoms reached the benthic layer in the model, they were converted to detritus and subjected to benthic remineralization. This nutrient source fed an increase in microflagellate production, leading to a maximum biomass of $> 1 \mu\text{mol C kg}^{-1}$ on 18 April in the model (Fig. 5(b)) despite high grazing rates (Table 1).

Upon subsequent atmospheric additions of iron-rich Saharan dust during June (Fig. 4), the simulated *T. erythraeum* populations increased by an order of magnitude within the water column, reaching a subsurface July–August maximum of $> 40 \mu\text{mol C kg}^{-1}$ or $\sim 2.5 \mu\text{g chl l}^{-1}$ (Fig. 6(c)). The opportunistic, fast growing diatom

population then assimilated these nutrients released by the diazotrophs, accumulating a biomass of $> 3 \mu\text{mol C kg}^{-1}$ in July (Fig. 6(a)). Once again, as observed in prior seasonal succession of phytoplankton on the WFS (Walsh et al., 2003), microflagellates followed in the model, with an August accumulation of $> 2 \mu\text{mol C kg}^{-1}$ (Fig. 6(b)), but only $\sim 0.4 \mu\text{g chl l}^{-1}$.

Nutrients recycled from the precursor diazotroph bloom (Fig. 6(c)) also fueled slow growth of *K. brevis*, which reached

specified fish killing concentrations of $> 4.5 \mu\text{mol C kg}^{-1}$, or $1.8 \mu\text{g chl l}^{-1}$, by late July (Fig. 6(d)). The simulated *K. brevis* population initially accumulated biomass near the bottom of the September water column (Fig. 6(d)), due to its low light saturation intensity (Table 1). This bottom development persisted, until sufficient biomass had accumulated to self-shade the HAB population. At this point, the early HAB of *K. brevis* migrated to the surface layer of the model, both concentrating and co-locating the red tide with positively buoyant dead fish by early October (Fig. 6(d)).

Simulated *K. brevis* stocks reached $\sim 12 \mu\text{mol C kg}^{-1}$ on 10 August, or $\sim 4.8 \mu\text{g chl l}^{-1}$ (Fig. 6(d)). This was similar to the chlorophyll biomass of the red tide as measured at this time on the inner WFS during 2001 (Vargo et al., 2004, 2008). Earlier on 28 July 2001, satellite imagery suggested a total phytoplankton stock of $8\text{--}10 \mu\text{g chl l}^{-1}$ at mid-shelf, compared to $1\text{--}2 \mu\text{g chl l}^{-1}$ on 3 July 2001 (Fig. 8).

Accordingly, this satellite time sequence was consistent with the model's surface estimates of the whole phytoplankton community of $\sim 7.4 \mu\text{g chl l}^{-1}$ on 10 August 2001, composed of $4.8 \mu\text{g chl l}^{-1}$ of *K. brevis*, $1.4 \mu\text{g chl l}^{-1}$ of *Trichodesmium*, $0.8 \mu\text{g chl l}^{-1}$ of diatoms, and $0.4 \mu\text{g chl l}^{-1}$ of microflagellates. Subsequently, *K. brevis* grew steadily throughout the fall on nutrients harvested from decaying fish and diazotrophs of the model, to surface stocks of $> 200 \mu\text{mol C kg}^{-1}$ in September, or $> 80 \mu\text{g chl l}^{-1}$ (Fig. 6(d)).

Satellite imagery of the phytoplankton community on 3 July (Fig. 8(a)) and 28 July 2001 (Fig. 8(b)) provided an initial assessment of the diazotrophs and dinoflagellates at the mid/inner shelf. On 3 July, *Trichodesmium* dominated the phytoplankton community. By 28 July, the optical signal (Carder et al., 2007; Cannizzaro et al., 2008) of *K. brevis* had become co-dominant with the diazotrophs, as observed during earlier red tides (Gunter et al., 1948; Walsh and Steidinger, 2001).

Once again, this successional sequence of phytoplankton, inferred from space, was consistent with model results. In response to ambient dFe and P stocks of the model and then deposition of Saharan dust during June–July, simulated growth of *Trichodesmium* led to population increments of ten-fold above background levels by late June 2001 and one hundred fold by late July (Fig. 6(c)), as observed then on the WFS (Lenos and Heil, 2010).

Little to no surface populations of *Trichodesmium* were present within shelf waters during April 2001, with initial detection of elevated biomass on the WFS during 15 June 2001. A maximum concentration of 3.0×10^6 trichomes l^{-1} was found on 15 July within surface waters of the inner shelf (Lenos and Heil, 2010).

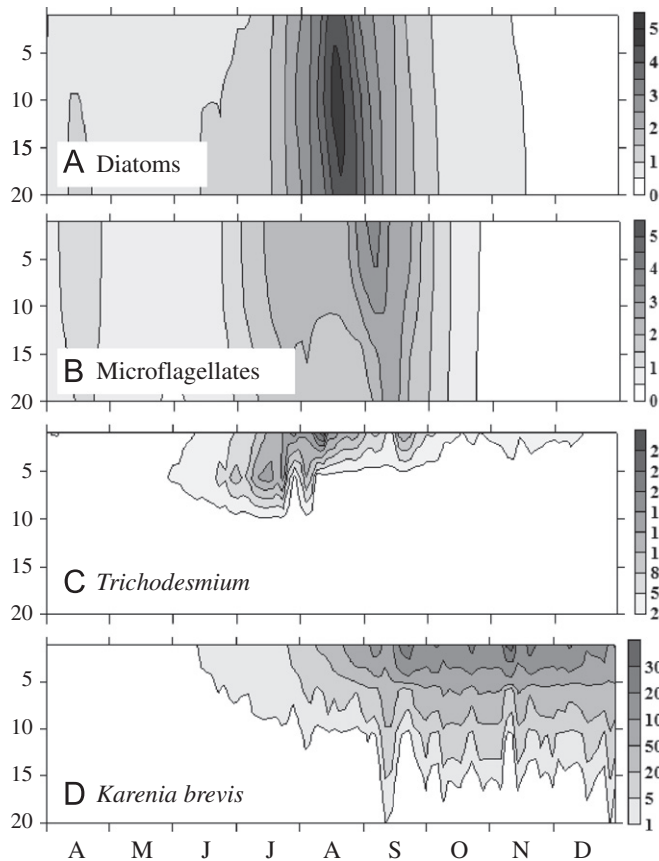


Fig. 6. The simulated daily phytoplankton concentration (mmol C m^{-3} or $\mu\text{mol C kg}^{-1}$) of (A) diatoms, (B) microflagellates, (C) *Trichodesmium*, and (D) *Karenia brevis* over the 20-m water column. Note change in scales.

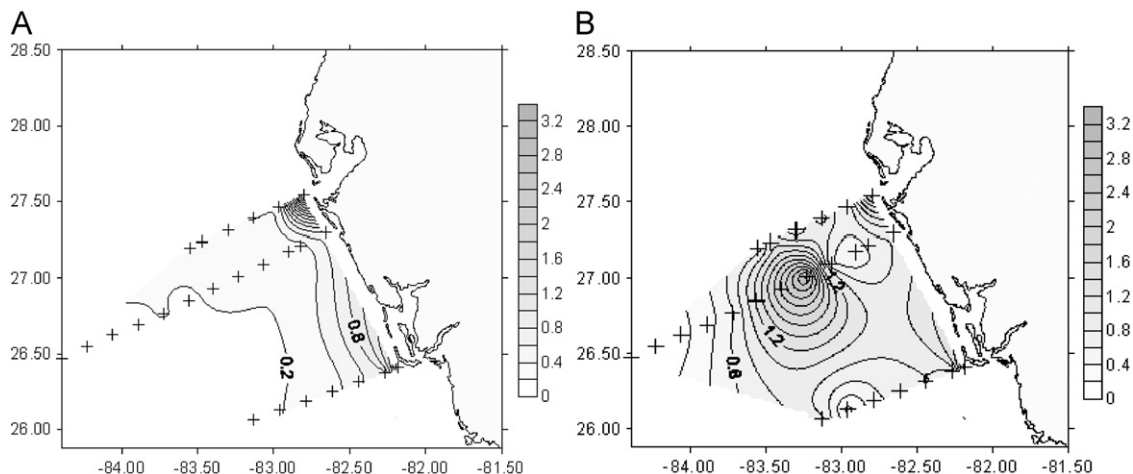


Fig. 7. Validation data of (A) near-surface and (B) near-bottom distributions of chlorophyll biomass ($\mu\text{g chl l}^{-1}$) of the total phytoplankton community on the WFS during 3–6 April 2001.

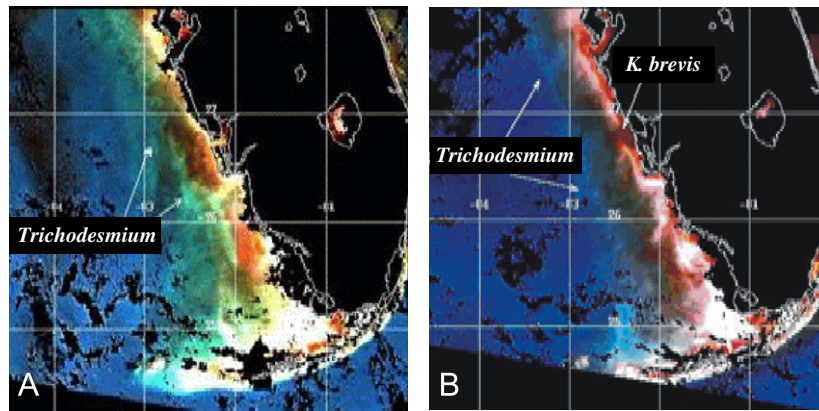


Fig. 8. The SeaWiFS satellite estimate of the optical properties of red tides and diazotrophs in the eastern Gulf of Mexico during (A) 3 July and (B) 28 July 2001. The reddish-black color in panel B is a red tide of *Karenia brevis* and the pale blue color in both panels is co-occurring *Trichodesmium*, based upon a backscatter algorithm (Carder et al., 2007; Cannizzaro et al., 2008). (For interpretation of the references to color in this figure legend, the reader is referred to the web version of this article.)

The observed maximum population was partially the result of frontal aggregation within wind rows. We were thus not surprised at the model's underestimate (Fig. 6(c)) from the 1-D simulations, given the present HABSIM's inability to aggregate biomass horizontally in a 3-D mode.

Simulated surface *K. brevis* stocks successfully reproduced the initiation and early maintenance of the observed *K. brevis* blooms, or weekly maxima (open circles of Fig. 9(a)), with an r^2 of 0.75 (Case 1a of Table 2) from 1 April–5 October 2001. Comparison of the baseline results of the model to the observed weekly maximal *K. brevis* concentrations yielded an MEF of 0.75 for Case 1a. These results demonstrated the model's ability to simulate changes of the surface biomass, as seen by satellites, in relation to vertical mixing of the population during wind events. For example, the decline in the surface biomass in early September (Fig. 9(a)) was accompanied by an increase in the near bottom population (Fig. 9(b)), not a decrease in the total integrated biomass.

Within the context of a 3-D “real world”, however, the vertical dispersion of HABs could be a significant factor in both termination and/or horizontal spreading of the bloom, in response to variations in the direction of transport at different depths (Weisberg and He, 2003). The 1-D version of HABSIM performed poorly in reproducing the termination of the surface *Karenia* HABs after 15 October 2001 (Fig. 9(a)). The baseline results of the model over the whole simulation period, from April to December 2001, had an r^2 of only 0.28, with an MEF of -0.46 (Case 1 of Table 2). The average error increased from 5.5 of Case 1a to 44.3 of Case 1 (Table 2).

There are several possibilities to explain this failure of long-term model fidelity, comprised – as usual – of unknown phytoplankton loss terms (Walsh, 1983). Previous simulations have indicated that advective losses, due to shifts in the prevailing winds, play a critical role in transport and dispersion of the surface *K. brevis* populations away from the coast (Weisberg et al., 2009; Walsh et al., 2009). Under conditions of thermal stratification, the shelf-wide upwelling/downwelling responses to synoptic winds are asymmetrical (Weisberg et al., 2001) and favor the shoreward progression and net retention of material properties in the bottom frictional boundary layer (Weisberg et al., 2009). It is also apparent that near-surface material tracers persist longer coherent patches or satellite-observed features during periods of thermal stratification (Jolliff et al., 2003, 2008). As the Gulf of Mexico basin-wide thermal stratification regularly breaks down in early October due to a decline in solar forcing and an increase

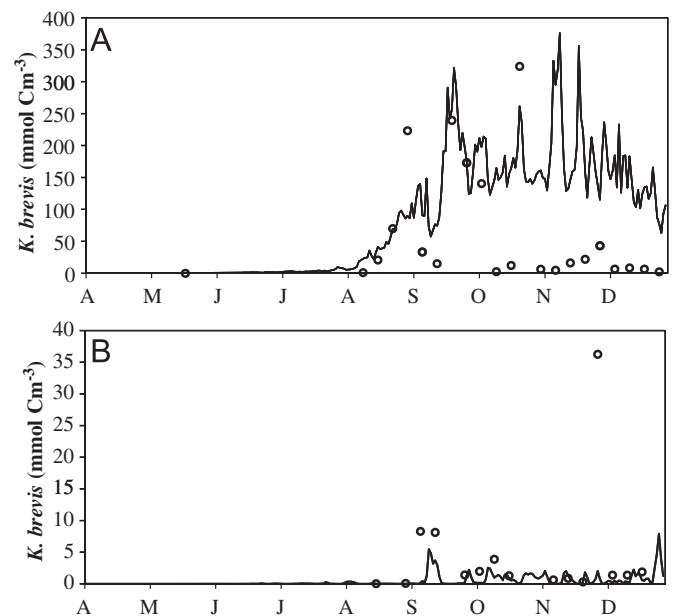


Fig. 9. The simulated daily baseline (Case 1) *Karenia brevis* concentrations (mmol C m^{-3} ; solid line) at the (A) surface and (B) near bottom layer in relation to the observed weekly maximum *Karenia brevis* concentrations (O) within 35 km of the West Florida coast between Cedar Key and Naples. Observed surface cell counts were collected at depths < 3 m and near bottom counts were collected between 15–20 m.

in episodic latent heat flux losses (Jolliff et al., 2008), the retentive asymmetry effects are likely diminished and more vigorous vertical mixing ensues. Thus after October 1, physical dispersion of any accumulated biomass patches in the “real world” were not captured in the 1-D model.

In addition, the model utilized constant loss terms of 1% grazing and 1% lysis per day (Table 1). It has been suggested that *K. brevis* is capable of programmed cell death under nutrient stress, viral lysis, and attack by algicidal bacteria (Doucette et al., 1999; Paul et al., 2002; Roth et al., 2008; Van Dolah et al., 2009), although the rates are yet to be quantified. Therefore, revisions of the loss term and coupling to a 3-D circulation model could compensate for the model's inability to reproduce bloom termination.

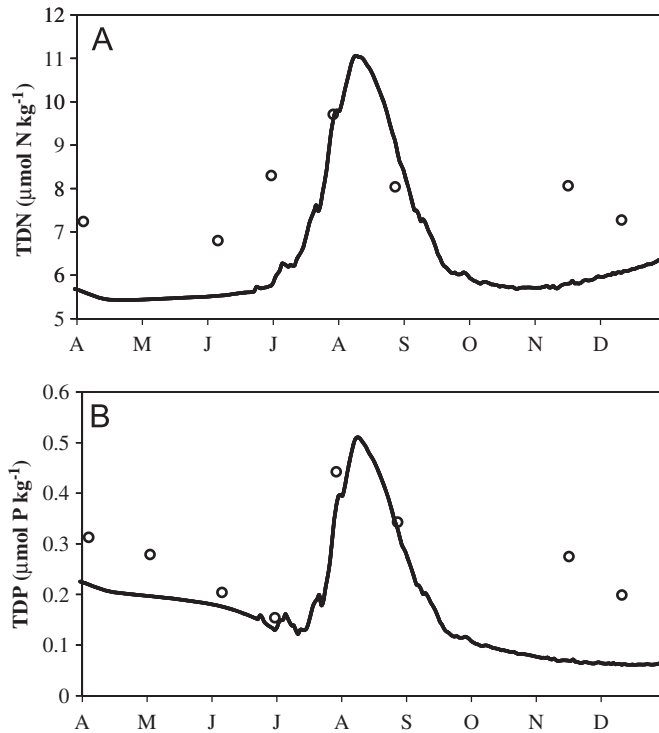


Fig. 10. The simulated daily surface concentrations ($\mu\text{mol kg}^{-1}$) of (A) Total Dissolved Nitrogen ($\text{TDN}=\text{NO}_3+\text{NH}_4+\text{DON}$) and (B) Total Dissolved Phosphorus ($\text{TDP}=\text{PO}_4+\text{DOP}$) in relation to the observed TDN and TDP at station 29 (27.2°N , -82.9°W) as measured during monthly ECOHAB cruises. Open circles represent field data while the solid lines are model results.

3.2. Nutrients

In early April 2001, the simulated surface TDN concentration of the baseline case was $\sim 5.8 \mu\text{mol N kg}^{-1}$ (Fig. 10(a)), somewhat elevated from earlier estimates of the mid-shelf background TDN concentrations of $\sim 5 \mu\text{mol N kg}^{-1}$ (Walsh et al., 2003). This model result was also consistent with the surface TDN concentration measured at station 29 on the 3–6 April 2001 ECOHAB cruise. We attribute these initial spring stocks of dissolved nitrogen off central Florida to nutrient sources from mainly the northern Gulf estuaries.

Subsequently, the simulated TDN increased 2-fold over the summer months to a maximum of $\sim 11.2 \mu\text{mol N kg}^{-1}$ by early August 2001 (Fig. 10(a)). Such an increment resulted from both N_2 fixation by *Trichodesmium* and decay of poisoned fish, with a nitrogen isotopic signature attributed to trophic transfers from nitrate-grown diatoms at base of their separate food chain (Walsh et al., 2009). Accordingly, the recycled DON of the model's baseline case (Fig. 11(f)) was responsible for the majority of this TDN increase.

The DON was quickly converted to NH_4 (Fig. 11(b)) and NO_3 (Fig. 11(a)) through bacterial processes of the model, where it became bioavailable for all components of the phytoplankton community. Increases in both the simulated diatom and microflagellate populations (Fig. 6(a) and (b)) directly resulted from this N supply. Thus, both the observed (open symbols of Fig. 11) and simulated nitrate stocks were usually less than $0.5 \mu\text{mol N kg}^{-1}$ during 2001. Although ammonium data were not available in 2001, the simulated seasonal maximum of $>0.2 \mu\text{mol N kg}^{-1}$ during August 2001 (Fig. 11(b)) was the same as those maximal amounts observed above the 10–50 m isobaths of the WFS during August 1998 and 1999 (Walsh et al., 2003).

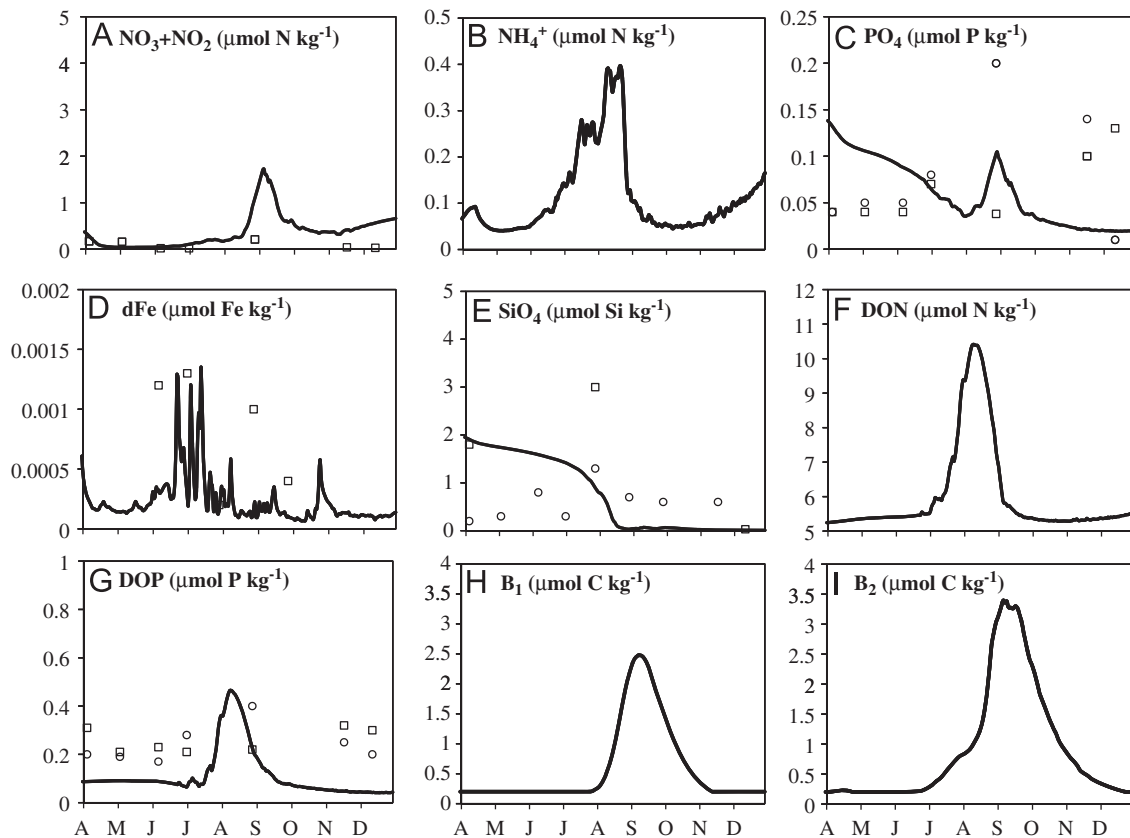


Fig. 11. The simulated daily surface concentration (—) and measured monthly isobath averages ($\square=10$ m; $\circ=25$ m) of (A) NO_3 , (B) NH_4 , (C) PO_4 , (D) dFe , (E) SiO_4 , (F) DON , (G) DOP , (H) ammonifying bacteria (B_1), and (I) nitrifying bacteria (B_2). Note change in scales.

Given the lack of a Si sources associated with the decay of *Trichodesmium* and dead fish, the diatoms quickly depleted the model's August SiO_4 concentrations to $<0.5 \mu\text{mol Si kg}^{-1}$ (Fig. 11(e)). This was again consistent with both the SiO_4 concentrations measured at the 10-m isobath, and to a lesser effect, at the 25-m isobaths during August 2001 (Fig. 9(e)), as well as during August 1998 and 1999 (Walsh et al., 2003). Note that the half-saturation constant for silica uptake by the diatoms was $0.5 \mu\text{mol Si kg}^{-1}$ in the model (Table 1). Therefore, the seasonal Si-limitation of the diatom population, together with the high grazing rates on the microflagellates kept both of their potentially fast-growing populations in check, allowing *K. brevis* to dominate the fall phytoplankton community (Fig. 6), despite the $10\times$ slower growth rates of the HABs.

While the simulated TDN pattern was consistent with the measured concentrations, the model still predicted a significant delay of phytoplankton biomass accumulations (~ 5 weeks), relative to those found at station 29. This discrepancy resulted from the model's underestimate of spring–summer stocks of DOP (Fig. 11(g)), and hence the slow initial growth of the modeled *Trichodesmium* population.

Competition for available P among the other phytoplankton and bacterial pools of the model had reduced the simulated DOP concentrations by 25–50%, relative to the observed concentrations at the 10-m and 25-m isobaths by the end of June 2001 (Fig. 11(g)). In contrast, the model correctly predicted the PO_4 at the end of that month (Fig. 11(c)). But, since DOP dominated the TDP pool (Fig. 10), such P-limitation suppressed *Trichodesmium*'s already slow growth

rate, despite sufficient Fe stocks by this date (Fig. 11(d)). Of course, if the model had instead employed a N/P regeneration ratio of 4, rather than 16, phosphorus limitation of *Trichodesmium* would have been much less, and the lag time of biomass accumulation would have only been ~ 9 day. Such sensitivity in the model to formulation of the “correct” N/P ratios of nutrient regeneration was shown in the highest sensitivity index (Fig. 5) of the C/P ratio of the *Karenia* HABs, followed by that of the growth rate, μ_3 , of *Trichodesmium* (Fig. 5).

3.3. Other model cases

In Case 2 of no river nutrient loadings, the model still predicted a *K. brevis* HAB with a surface value of $\sim 225 \text{ mmol C m}^{-3}$ on 15 September 2001 (Fig. 12(a)), compared to $\sim 325 \text{ mmol C}$ on the same day of the baseline case (Fig. 9(a)). A few days earlier, a similar amount of $\sim 250 \text{ mmol C m}^{-3}$ of near-surface dinoflagellate stock had been observed that month on the WFS (Fig. 9(a)). This reduction of only 30% between the two model cases, which bracketed the observations, suggested that the spring nutrient inputs from the northern estuaries and remineralization of the subsequent diatom population were not causative agents of red tides on the WFS. These model results instead reflected the secondary role of dead fish produced in this parallel food chain for the maintenance, but not the initiation of red tides (Walsh et al., 2009). This decreased model fidelity was confirmed by an overall r^2 of 0.14 for Case 2, compared to one of 0.28 for Case 1 (Table 2).

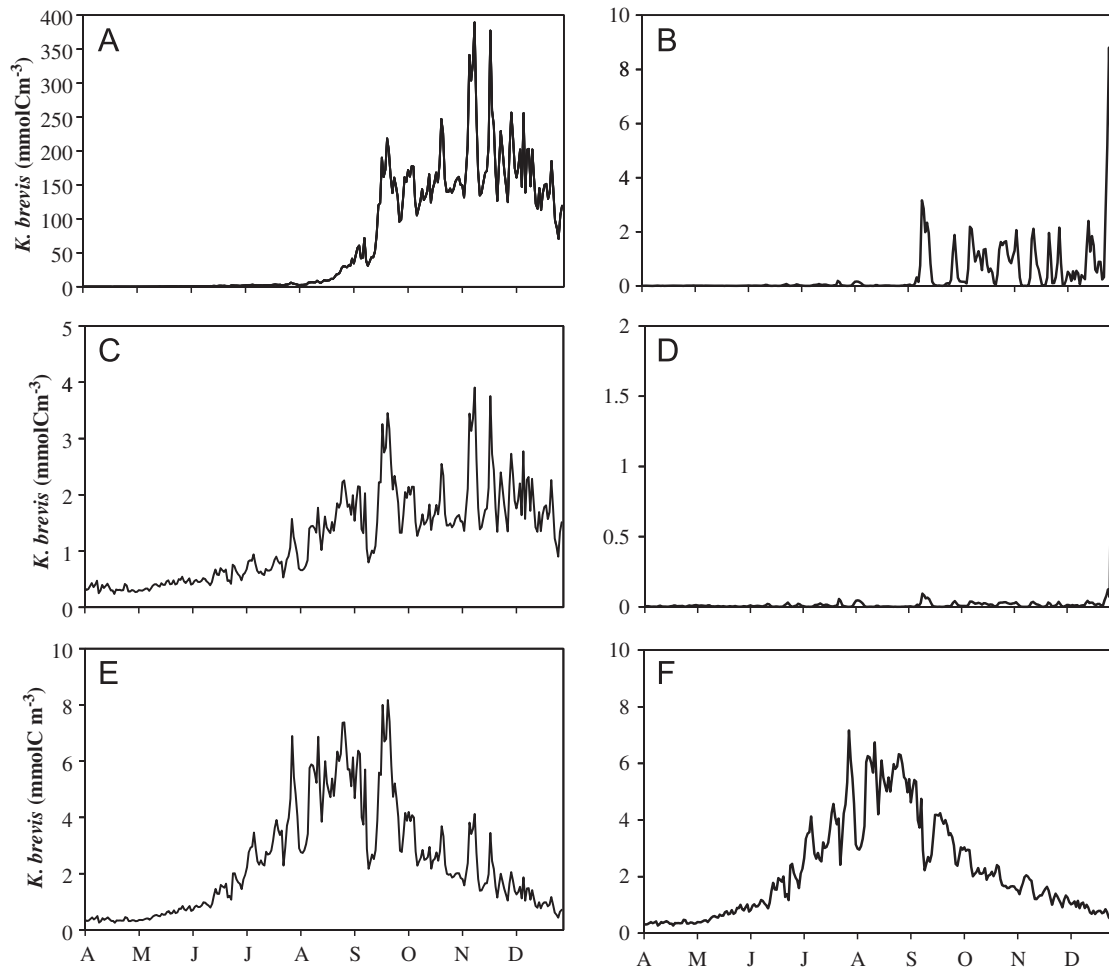


Fig. 12. The simulated daily *Karenia brevis* concentrations (mmol C m^{-3}) for Case 2 (no river pulse) within the (A) surface and (B) near bottom layers, for Case 3 (no *Trichodesmium*) within the same (C), (D) layers; and for Case 4 (no dead fish) within the same (E), (F) layers. Note change in scales.

The removal of N_2 fixers in Case 3 led to an insignificant red tide of *K. brevis* on 15 October 2001 of $< 2.5 \text{ mmol C m}^{-3}$ within surface waters of the model (Fig. 12(c)). Ambient nutrient stocks supported slow growth of *K. brevis*, reaching a maximum surface concentration of $\sim 4 \text{ mmol C m}^{-3}$ by early November. While this HAB concentration would have been large enough to force closures of commercial harvests from shellfish beds, the red tides of the model then did not exceed those levels needed to cause significant fish kills.

Similarly, the removal of dead fish in Case 4 restricted the maximum simulated concentration of *K. brevis* to $\sim 2.7 \text{ mmol C m}^{-3}$ on 15 October 2001 (Fig. 12(e)). After this date, the absence of a dead fish maintenance supply of nutrients led to an accumulated HAB of only $0.8 \text{ mmol C m}^{-3}$ by 31 December 2001 in Case 3 (Fig. 12(e)), compared to $1.5 \text{ mmol C m}^{-3}$ on the same day in case 2 (Fig. 12(c)). Recall that very small amounts of *K. brevis* were also observed near the sea surface on that day (Fig. 9(a)), but presumably as a result of advective and/or grazing losses, not in response to meager supplies of recycled nutrients. The last sensitive parameter of the model was that of grazing stress, λ_4 , on *K. brevis* (Fig. 5), which can vary tenfold from one year to the next on the WFS (Walsh et al., 2011a).

4. Discussion

In a shallow WFS water column of 20 m, rapid sinking velocities of diatom blooms (Walsh and Dieterle, 1994) and zooplankton fecal pellets (Walsh et al., 2003) ensured arrival of phytodetritus and egested herbivore debris in less than one day. Based on conventional wisdom, the grazing fluxes, λP , varied for each phytoplankton state variable, as a function of their assessed palatability to copepods and protozoans. When herbivores are explicit state variables of a model (Walsh, 1976), they provide both grazing closure and/or linkage to other components of the coastal food web.

With respect to grazing on *K. brevis* by copepods, the crustaceans are thought to be ineffective herbivores of these HABs by observationalists (Kleppel et al., 1996; Turner and Tester, 1997; Lester et al., 2008). Yet, grazing controls are exerted by calanoid copepod herbivores on the WFS in numerical models, albeit on diatoms not toxic dinoflagellates (Milroy et al., 2008). Indeed, the clupeid fish, which *K. brevis* harvests as a supplemental nutrient source (Walsh et al., 2009), are supported by a short parallel food chain, based in turn on spring blooms of diatoms, mainly *Skeletonema costatum* (Saunders and Glenn, 1969), eaten by calanoid copepods. Furthermore, based on their specific rates of grazing (Dagg, 1995) and observed abundances during September 1998, copepod herbivores may then have consumed as much as 50% of the daily production (Sutton et al., 2001) of the previous near-bottom summer diatom stocks of $3\text{--}4 \mu\text{g chl l}^{-1}$ on the middle WFS.

By late fall, however, no diatom food was left for the surviving copepods (Walsh et al., 2003). These facultative herbivores must instead consume first protozoans (Kleppel et al., 1996), and then populations of *K. brevis* in the “real world”. Indeed, with no alternative diatom prey, the copepods will eat these toxic dinoflagellates in coastal waters (Turner and Tester, 1997), preventing accumulation of ungrazed toxic summer red tides on the WFS (Milroy et al., 2008) of $> 1 \mu\text{g chl l}^{-1}$, as was observed in 1966, 1972, 1993, 1998, and 2000 (Walsh et al., 2006).

On the 30-m isobath off Sarasota and Tampa, FL, for example, the dominant copepod genera were *Paracalanus*, *Temora*, *Centropages*, *Oithona*, *Oncaea*, and *Corycaeus* in both September 1998 (Sutton et al., 2001) and 1999 (Lester et al., 2008). Although these copepods generally shun *K. brevis* (Tester et al., 2000), the dominant smaller WFS calanoid

copepods, e.g., *P. quasimodo*, will eat this HAB, if no other prey are available, within downstream North Carolina shelf waters (Turner and Tester, 1997). Moreover, long-term changes of the phytoplankton abundances and species composition on the WFS have been attributed to reduced grazing pressures, after increased consumption of the herbivores by zooplanktivores during trophic cascades (Walsh et al., 2011a).

Yet, these parameters of algal palatability were just implicit fixed rates of phytoplankton abundances in the present 1-D simulations. No consideration was given to the explicit population dynamics of the zooplankton herbivores, which both eat these microalgae and, in turn, are subject to predation by clupeid and chaetognath carnivores. Proper grazing stress formulations are thus required in future models, as well as time-dependent nutrient regeneration formulations and algal lysis, to accurately derive species succession and HAB maintenance within the context of 3-D physical dispersion loss terms as part of the mechanisms driving bloom termination.

The Coastal Ocean Monitoring System (COMPS) at the University of South Florida (USF) was developed as part of the Regional Coastal Ocean Observing System (RCOOS) for the southeastern United States (Weisberg et al., 2009). The past COMPS consisted of tide gauges, surface meteorological sensors, buoys with acoustic Doppler current profilers (ADCPs), temperature (T) and salinity (S) sensors, high frequency radar for surface current mapping, and bottom stationed ocean profilers (BSOPs) for discrete measurements of T, S, and chlorophyll fluorescence at a few locations (see <http://ocgweb.marine.usf.edu>). Such COMPS data, supplemented with glider observations could now provide both the offshore boundary conditions and validation criteria for real-time improvements of the fidelity of future operational HAB models. With revisions to a 3-D version of HABSIM, including time-dependent N/P remineralization ratios, explicit herbivore state variables, and physical dispersion losses, we will next explore the reasons for the large HAB of 2001, compared to the small ones of 2007 and 2009 (Walsh et al., 2009; 2011a).

5. Conclusion

One-dimensional simulations using the ecological model, HABSIM, indicated that late summer/fall blooms of the toxic dinoflagellate, *Karenia brevis*, was initiated in response to nitrogen fixation by the colonial cyanophyte, *Trichodesmium erythraeum*, on the WFS, not in response to upwelled or riverine sources of nutrients. Instead, these deep water and freshwater inputs supported a more typical diatom–copepod–clupeid food web. Once, *K. brevis* blooms reached concentrations $> 4.5 \mu\text{mol C kg}^{-1}$, they were capable of both self-shading and causing extensive mortality of higher trophic levels. The combination of these decaying top level predators and mortality of the lower trophic *Trichodesmium* populations supplied additional non-siliceous N and P sources for use by these HABs. This provided a competitive advantage for further development and maintenance of the slow-growing *K. brevis* population over the faster growing diatoms and microflagellates. While a monospecific bloom of *K. brevis* at concentrations $> 5 \times 10^5 \text{ cells l}^{-1}$ would take advantage of any and all nutrient sources they encounter, the causal model's specified chain of events was necessary to reach the observed cellular concentrations of red tides off western Central Florida (Fig. 1). We are thus ready to implement this model, in conjunction with COMPS for development of an operational model of the trophodynamics of red tides, fish yields, and perturbation

responses in the eastern GOM to climate change, overfishing, and oligotrophication.

6. Math formulae

Diatoms:

$$\frac{\partial dP_1}{\partial t} = Tr_t(dP_1) - \frac{\partial}{\partial \sigma} w_1 P_1 + dg_1 P_1 - d\gamma_1 P_1 - d\varepsilon_1 P_1 - d\psi_1 P_1 - dl_1 P_1$$

Microflagellates:

$$\frac{\partial dP_2}{\partial t} = Tr_t(dP_2) + dg_2 P_2 - d\gamma_2 P_2 - d\varepsilon_2 P_2 - d\psi_2 P_2 - dl_2 P_2$$

Trichodesmium:

$$\frac{\partial dP_3}{\partial t} = Tr_t(dP_3) - \frac{\partial}{\partial \sigma} (w_3 P_3) + dg_3 P_3 - d\gamma_3 P_3 - d\varepsilon_3 P_3 - dl_3 P_3$$

K. brevis:

$$\frac{\partial dP_4}{\partial t} = Tr_t(dP_4) - \frac{\partial}{\partial \sigma} (w_4 P_4) + dg_4 P_4 - d\gamma_4 P_4 - d\varepsilon_4 P_4 - dl_4 P_4$$

Ammonifiers:

$$\frac{\partial dB_a}{\partial t} = Tr_t(dB_a) + dg_a B_a - d\varepsilon_a B_a - dm_a B_a$$

Nitrifiers:

$$\frac{\partial dB_n}{\partial t} = Tr_t(dB_n) + dg_n B_n - d\varepsilon_n B_n - dm_n B_n$$

Dissolved iron:

$$\begin{aligned} \frac{\partial dFe_d}{\partial t} = & Tr_t(dFe_d) + d[(Fe : C)_{1-4}(\varepsilon_{1-4} P_{1-4}) - (g_{1-4} P_{1-4}) + (\gamma_{1-4} \varepsilon_{\gamma_{1-4}})] \\ & + d\beta_{Fe} - d\alpha_{Fe} + d[(Fe : C)_{1-4}(\varepsilon_f \gamma_{1-4} f_{\gamma_{1-4}})] + d\kappa_{Fe} \end{aligned}$$

Ammonium:

$$\begin{aligned} \frac{\partial dNH_4}{\partial t} = & Tr_t(dNH_4) + d(N : C)_{1-4}(\varepsilon_{1-4} P_{1-4} - g_{1,2,4} P_{1,2,4} + \gamma_{1-4} P_{1-4}) \\ & + d(N : C)_b(\varepsilon_{B_a} g_a B_a - g_n B_n) + d\beta_{DON} + d(N : C)_{1-4} \varepsilon_f \gamma_f f_{\gamma_{1-4}} \end{aligned}$$

Nitrate:

$$\frac{\partial dNO_3}{\partial t} = Tr_t(dNO_3) - d(N : C)_{1-4} g_{1-4} P_{1-4} + d\varepsilon_{B_n} g_n B_n$$

Phosphate:

$$\begin{aligned} \frac{\partial dPO_4}{\partial t} = & Tr_t(dPO_4) + d(P : C)_{1-4}(\varepsilon_{1-4} P_{1-4} - g_{1-4} P_{1-4} + \gamma_{1-4} P_{1-4}) \\ & + d(P : C)_b(\varepsilon_{B_a} g_a B_a + \varepsilon_{B_n} g_n B_n - g_n B_n) + d\beta_{DOP} \\ & + d(P : C)_{1-4} \varepsilon_f \gamma_f f_{\gamma_{1-4}} \end{aligned}$$

Detritus:

$$\frac{\partial dD}{\partial t} = Tr_t(dD) - \frac{\partial}{\partial \sigma} (w_D D) + dq_{1-4} l_{1-4} - dk_D D$$

Fecal pellets:

$$\frac{\partial dZ}{\partial t} = Tr_t(dZ) - \frac{\partial}{\partial \sigma} (w_Z Z) + dA_{1-4} \gamma_{1-4} + d\gamma_{1-5} b_{1-5} f - dk_Z Z$$

Silicate:

$$\begin{aligned} \frac{\partial dSiO_4}{\partial t} = & Tr_t(dSiO_4) + d(Si : C)_1(\varepsilon_1 P_1 - g_1 P_1 + \lambda_1 P_1) \\ & + dk_{diss}(Si : C)_1(Z + D) \end{aligned}$$

DON:

$$\begin{aligned} \frac{\partial dDON}{\partial t} = & Tr_t(dDON) + d(N : C)_{1-4}(\sigma_{1-4} l_{1-4} P_{1-4} + j_{1-4} \gamma_{1-4} P_{1-4}) \\ & + d(N : C)_b(m_a B_a + m_n B_n - g_a B_a) + d(N : C)_{1-4}(k_D D + k_Z Z) \\ & - d\beta_{DON} + d(N : C)_{1-4} k_{fd} F \end{aligned}$$

DOP:

$$\begin{aligned} \frac{\partial dDOP}{\partial t} = & Tr_t(dDOP) + d(P : C)_{1-4}(\sigma_{1-4} l_{1-4} P_{1-4} + j_{1-4} \gamma_{1-4} P_{1-4}) \\ & + d(P : C)_b(m_a B_a + m_n B_n - g_a B_a) + d(P : C)_{1-4}(k_D D + k_Z Z) \\ & - d\beta_{DOP} + d(P : C)_{1-4} k_{fd} F \end{aligned}$$

DOC:

$$\begin{aligned} \frac{\partial dDOC}{\partial t} = & Tr_t(dDOC) + d(\sigma_{1-4} l_{1-4} P_{1-4} + j_{1-4} \gamma_{1-4} P_{1-4}) \\ & + d(m_a B_a + m_n B_n - g_a B_a) + d(k_D D + k_Z Z) - d\beta_{DOC} + dk_{fd} F \end{aligned}$$

Colloidal iron:

$$\begin{aligned} \frac{\partial dFe_c}{\partial t} = & Tr_t(dFe_c) + d(Fe : C)_{1-4}(\sigma_{1-4} l_{1-4} P_{1-4} + j_{1-4} \gamma_{1-4} P_{1-4}) \\ & + d(Fe : C)_{1-4}(k_D D + k_Z Z) - d\beta_{Fe} + d\alpha_{Fe} + d(Fe : C)_{1-4} k_{fd} F \end{aligned}$$

DIC:

$$\begin{aligned} \frac{\partial dDIC}{\partial t} = & Tr_t(dDIC) + d(\varepsilon_{1-4} P_{1-4} - g_{1-4} P_{1-4} + \gamma_{1-4} P_{1-4}) \\ & + d(\varepsilon_{B_a} g_a B_a + \varepsilon_{B_n} g_n B_n - g_n B_n) + d\varepsilon_f \gamma_{1-4} f_{\gamma_{1-4}} \end{aligned}$$

Fish:

$$\frac{\partial dZP}{\partial t} = Tr_t(dZP) + d\gamma_{1-4} f_{\gamma_{1-4}} P_{1-4} b_{1-4} - dk_{fd} ZP - \frac{\partial}{\partial \sigma} w_f ZP$$

Diffusive transport:

$$Tr_t(dQ) = \frac{k_h}{d} \frac{\partial Q}{\partial \sigma}$$

Diatom growth:

$$g_1 = [\mu_1] \left[\begin{array}{l} \min(I_z/I_{sat} e^{(1-I_z/I_{sat}(1))}), (NO_3/\{k_{NO_3(1)} + NO_3\}), \\ \text{or } (NH_4/\{k_{NH_4(1)} + NH_4\}), (PO_4/\{k_{PO_4(1)} + PO_4\}), \\ (SiO_4/\{k_{SiO_4(1)} + SiO_4\}) \end{array} \right]$$

Microflagellate growth:

$$g_2 = [\mu_2] \left[\begin{array}{l} \min(I_z/I_{sat} e^{(1-I_z/I_{sat}(2))}), (NO_3/\{k_{NO_3(2)} + NO_3\}), \\ \text{or } (NH_4/\{k_{NH_4(2)} + NH_4\}), (PO_4/\{k_{PO_4(2)} + PO_4\}) \end{array} \right]$$

Trichodesmium growth:

$$g_3 = [\mu_3] \left[\begin{array}{l} \min(I_z/I_{sat} e^{(1-I_z/I_{sat}(3))}), (PO_4/\{k_{PO_4(3)} + PO_4\}), \\ \text{or } (DOP/\{k_{DOP(3)} + DOP\}), (Fe_d/\{k_{Fe_d(3)} + Fe_d\}) \end{array} \right]$$

K. brevis growth:

$$g_4 = [\mu_4] \left[\begin{array}{l} \min(I_z/I_{sat} e^{(1-I_z/I_{sat}(4))}), (NO_3/\{k_{NO_3(4)} + NO_3\}), \\ \text{or } (NH_4/\{k_{NH_4(4)} + NH_4\}) \text{ or } (DON/\{k_{DON(4)} + DON\}), \\ (PO_4/\{k_{PO_4(2)} + PO_4\}) \text{ or } (DOP/\{k_{DOP(4)} + DOP\}), (Fe_d/\{k_{Fe_d(4)} + Fe_d\}) \end{array} \right]$$

Maximal growth rate:

$$\mu_{1-4} = \mu_{t(1-4)} e^{0.0633(T-27)}$$

Ammonifier growth:

$$g_a = [\mu_a] [\min(DON/\{k_{DON(a)} + DON\}), (DOP/\{k_{DOP(a)} + DOP\})]$$

Nitrifier growth:

$$g_n = [\mu_n] [\min(NH_4/\{k_{NH_4(n)} + NH_4\}), (PO_4/\{k_{PO_4(n)} + PO_4\})]$$

Fish decay:

$$k_{fd} = 1.97 \times 10^{-1} \cdot T$$

Iron scavenging:

$$\alpha_{fe} = \alpha_{\max} Fe_d (Fe_d / (Fe_d + k_z))$$

Trichodesmium lysis:

$$\kappa = [\min(PO_4/(k_{PO_4(3)} + PO_4)), \\ \text{or } (DOP/(k_{DOP(3)} + DOP))], (Fe_d/(k_{Fe_d(3)} + Fe_d)) \\ l_3 = P_3 l_{\max} e^{-13.54\kappa}$$

Acknowledgments

This analysis was supported by grants NA16OP2787 to JJW and RHW from the National Oceanic and Atmospheric Administration as part of the MERHAB program; NA06NOS4780246 to JJW and RHW as part of the ECOHAB:Karenia program; NNX09AT48G to JML from the National Aeronautics and Space Administration Applied Sciences; and grant #07170 to JML from the Florida Fish and Wildlife Commission Red Tide Control and Mitigation program. This is ECOHAB contribution #657, MERHAB contribution #151 and CPR contribution #15. In particular, we would also like to thank Joseph Prospero for providing dust data, FWC for the *K. brevis* data and the ECOHAB:Florida project and associated participants for the nutrient data.

References

- Anderson, T.R., 2005. Plankton functional type modelling: running before we can walk. *Journal of Plankton Research* 27, 1073–1081.
- Austin, H.M., Jones, J.L., 1974. Seasonal variation of physical oceanographic parameters on the Florida Middle Ground and their relation to zooplankton biomass on the West Florida shelf. *Florida Scientist* 37, 16–32.
- Baden, D.G., Mende, T.J., 1979. Amino acid utilization by *Gymnodinium breve*. *Phytochemistry* 18, 247–251.
- Barth, A., Alvera-Azcarate, A., Weisberg, R.H., 2008. Benefit of nesting a regional model into a large-scale ocean model instead of climatology: application to the West Florida shelf. *Continental Shelf Research* 28, 561–573.
- Berman-Frank, I., Bidle, K.D., Haramaty, L., Falkowski, P.G., 2004. The demise of the marine cyanobacterium *Trichodesmium* spp., via an autocatalyzed cell death pathway. *Limnology and Oceanography* 49, 997–1005.
- Berman-Frank, I., Rosenberg, G., Levitan, O., Haramaty, L., Mari, X., 2007. Coupling between autocatalytic cell death and transparent exopolymeric particle production in the marine cyanobacterium *Trichodesmium*. *Environmental Microbiology* 9, 1415–1422.
- Biber, P.D., Harwell, M.A., Cropper Jr., W.P., 2004. Modeling the dynamics of three functional groups of macroalgae in tropical seagrass habitats. *Ecological Modelling* 175, 25–54.
- Bledsoe, E.L., Philips, E.J., 2000. Relationships between phytoplankton standing crop and physical, chemical, and biological gradients in the Suwannee River and plume region, USA. *Estuaries* 23, 458–473.
- Brand, L.E., Compton, A., 2007. Long-term increase in *Karenia brevis* abundance along the southwest Florida coast. *Harmful Algae* 6, 232–252.
- Cannizzaro, J.P., Carder, K.L., Chen, F.R., Heil, C.A., Vargo, G.A., 2008. A novel technique for detection of the toxic dinoflagellate, *Karenia brevis*, in the Gulf of Mexico from remotely sensed ocean color data. *Continental Shelf Research* 28, 137–158.
- Carder, K.L., Walsh, J.J., Cannizzaro, J.P., 2007. Hunting red tides from space. In: King, M.D., Parkinson, C.L., Partington, K.C., Williams, R.G. (Eds.), *Our Changing Planet*. Cambridge University Press, Cambridge, pp. 187–190.
- Carpenter, E.J., 1983. Nitrogen fixation by marine *Oscillatoria* (*Trichodesmium*) in the world's oceans. In: Carpenter, E.J., Capone, D.G. (Eds.), *Nitrogen in the Marine Environment*. Elsevier, New York, pp. 65–103.
- Carpenter, E.J., Roenneberg, T., 1995. The marine planktonic cyanobacterium *Trichodesmium* spp.: photosynthetic rate measurements in the SW Atlantic Ocean. *Marine Ecology-Progress Series* 118, 267–273.
- Chassignet, E.P., Smith, L.T., Halliwell, G.R., Bleck, R., 2003. North Atlantic simulation with the HYbrid Coordinate Ocean Model (HYCOM): impact of the vertical coordinate choice, reference density, and thermobaricity. *Journal of Physical Oceanography* 33, 2504–2526.
- Dagg, M.J., 1995. Copepod grazing and the fate of phytoplankton in the northern Gulf of Mexico. *Continental Shelf Research* 15, 1303–1317.
- Darrow, B.P., Walsh, J.J., Vargo, G.A., Masserini, R.T., Fanning, K.A., Zhang, J.Z., 2003. A simulation study of the growth of benthic microalgae following the decline of a surface phytoplankton bloom. *Continental Shelf Research* 23, 1265–1283.
- Darrow, B.P., 2008. Effects of Nutrients from the Water Column on the Growth of Benthic Microalgae in Permeable Sediments. Ph.D. Dissertation. University of South Florida.
- del Giorgio, P.A., Cole, J.J., 2000. Bacterial energetics and growth efficiency. In: Kirchman, D.L. (Ed.), *Microbial Ecology of the Oceans*. John Wiley & Sons, New York, pp. 289–325.
- Dennison, W.C., Abal, E.G., 1999. Moreton Bay study: a scientific basis for the Healthy Waterways Campaign. South East Queensland Regional Water Quality Management Strategy, Brisbane 1–246.
- Dortch, Q., Whitledge, T.E., 1992. Does nitrogen or silicon limit phytoplankton production in the Mississippi River plume and nearby regions? *Continental Shelf Research* 12, 1293–1309.
- Dortch, Q., Robichaux, R., Pool, S., Milsted, D., Mire, G., Rabalais, N.N., Soniat, T.M., Fryxell, G.A., Turner, R.E., Parsons, M.L., 1997. Abundance and vertical flux of *Pseudonitzschia* in the northern Gulf of Mexico. *Marine Ecology Progress Series* 146, 249–264.
- Ducklow, H., 2000. Bacterial and biomass production in the oceans. In: Kirchman, D.L. (Ed.), *Microbial Ecology of the Oceans*. John Wiley & Sons, New York, pp. 85–120.
- Doucette, G.J., McGovern, E.R., Babinchak, J.A., 1999. Bacterial influences on HAB population dynamics. Part 1. Algalicidal bacteria active against the Florida red tide dinoflagellate, *Gymnodinium breve*. *Journal of Phycology* 35, 1447–1454.
- Fahnenstiel, G.L., McCormick, M.J., Lang, G.A., Redalje, D.G., Lohrenz, S.E., Markowitz, M., Wagoner, B., Carrick, H.J., 1995. Taxon-specific growth and loss rates for dominant phytoplankton populations from the northern Gulf of Mexico. *Marine Ecology-Progress Series* 117, 229–239.
- Fasham, M.J.R., Ducklow, H.W., McKelvie, M., 1990. A nitrogen based model of plankton dynamics in the oceanic mixed layer. *Journal of Marine Research* 48, 591–639.
- Flynn, K.J., 2005. Castles built on sand: dysfunctionality in plankton models and the inadequacy of dialogue between biologists and modellers. *Journal of Plankton Research* 27, 1205–1210.
- Franks, P.J.S., Wroblewski, J.S., Flierl, G.R., 1986. Behavior of a simple plankton model with food-level acclimation by herbivores. *Marine Biology* 91, 121–129.
- Friedrichs, M.A.M., Dusenberry, J.A., Anderson, L.A., Armstrong, R.A., Chai, F., Christian, J.R., Doney, S.C., Dunne, J., Fujii, M., Hood, R., McGillicuddy, D.J., Moore, J.K., Schartau, M., Spitz, Y.H., Wiggert, J.D., 2007. Assessment of skill and portability in regional marine biogeochemical models: role of multiple planktonic groups. *Journal of Geophysical Research* 112, C08001, <http://dx.doi.org/10.1029/2006JC003852>.
- Friedrichs, M.A.M., Carr, M.E., Barber, R.T., Scardi, M., Antoine, D., Armstrong, R.A., Asanuma, I., Behrenfeld, M.J., Buitenhuis, E.T., Chai, F., Christian, J.R., Ciotti, A.M., Doney, S.C., Dowell, M., Dunne, J., Gentili, B., Gregg, W., Hoepffner, N., Ishizaka, J., Kameda, T., Lima, I., Marra, J., Mélin, F., Moore, J.K., Morel, A., O'Malley, R.T., O'Reilly, J., Saba, V.S., Schmelz, M., Smyth, T.J., Tjiputra, J., Waters, K., Westberry, T.K., Winguth, A., 2009. Assessing the uncertainties of model estimates of primary productivity in the tropical Pacific Ocean. *Journal of Marine Systems* 76, 113–133.
- Geesey, M., Tester, P.A., 1993. *Gymnodinium breve*: ubiquitous in Gulf of Mexico waters?. In: Smayda, T.J., Shimizu, Y. (Eds.), *Toxic Phytoplankton Blooms in the Sea*. Elsevier, Amsterdam, pp. 251–255.
- Gilbes, F., Tomas, C.R., Walsh, J.J., Muller-Karger, F.E., 1996. An episodic chlorophyll plume on the West Florida shelf. *Continental Shelf Research* 16, 1201–1224.
- Gilbes, F., Müller-Karger, F.E., Del Castillo, C.E., 2002. New evidence for the West Florida shelf plume. *Continental Shelf Research* 22, 2479–2496.
- Glibert, P.M., Terlizzi, D.E., 1999. Co-occurrence of elevated urea levels and dinoflagellate blooms in temperate estuarine aquaculture ponds. *Applied and Environmental Microbiology* 65, 5594–5596.
- Grill, E.V., Richards, F.A., 1964. Nutrient regeneration from phytoplankton decomposing in seawater. *Journal of Marine Research* 22, 51–69.
- Gunter, G., Williams, R.H., Davis, C.C., Smith, F.G., 1948. Catastrophic mass mortality of marine animals and coincident phytoplankton bloom on the west coast of Florida, November 1946 to August 1947. *Ecological Monographs* 18, 309–324.
- Guo, C., Tester, P.A., 1994. Toxic effect of the bloom-forming *Trichodesmium* sp. (Cyanophyta) to the copepod *Acartia tonsa*. *Natural Toxins* 2, 222–227.
- He, R., Weisberg, R.H., 2002. West Florida shelf circulation and temperature budget for the 1999 spring transition. *Continental Shelf Research* 22, 719–748.
- Heil, C.A., Mulholland, M.R., Bronk, D.A., Bernhardt, P., O'Neil, J.M., 2004. Bacterial and size fractionated primary production within a *Karenia brevis* bloom on the West Florida shelf. In: Steidinger, K.A., Landsberg, J.H., Tomas, C.R., Vargo, G.A. (Eds.), *Harmful Algae 2002*. Florida Fish and Wildlife Commission, Florida Institute of Oceanography, and Intergovernmental Oceanographic Commission of UNESCO, St. Petersburg, FL, pp. 38–40.
- Heil, C.A., Revilla, M., Glibert, P.M., Murasko, S., Alexander, J., 2007. Nutrient quality drives phytoplankton community composition on the Southwest Florida shelf. *Limnology and Oceanography* 52, 1067–1078.
- Heil, C.A., Steidinger, K., 2008. Monitoring, management, and mitigation of *Karenia* blooms in the eastern Gulf of Mexico. *Harmful Algae* 8, 611–617.
- Hitchcock, G.L., Vargo, G.A., Dickson, M.L., 2000. Plankton community composition, production, and respiration in relation to dissolved inorganic carbon on the West Florida shelf. *Journal of Geophysical Research* 105, 6579–6589.
- Hood, R.R., Laws, E.A., Armstrong, R.A., Bates, N.R., Brown, C.W., Carlson, C.A., Chai, F., Doney, S.C., Falkowski, P.G., Feely, R.A., Friedrichs, M.A.M., Landry, M.R., Moore, J.K., Nelson, D.M., Richardson, T.J., Salihoglu, B., Schartau, M., Toole, D.A., Wiggert, J.D., 2006. Pelagic functional group modeling: progress, challenges and prospects. *Deep Sea Research Part II* 53, 459–512.
- Houde, E.D., Chitty, N., 1976. Seasonal Abundance and Distribution of Zooplankton, Fish Eggs, and Fish Larvae in the Eastern Gulf of Mexico, 1972–74. NOAA Technical Report. NMFS SSRF-701. Seattle WA, pp. 1–18.
- Houde, E.D., Leak, J.C., Dowd, C.E., Berkeley, S.A., Richards, W.J., 1979. Ichthyoplankton abundance and diversity in the eastern Gulf of Mexico. *USDOC NTIS PB-299 839*, pp. 1–546.

- Hu, C., Muller-Karger, F.E., Swarzenski, P.W., 2006. Hurricanes, submarine ground-water discharge, and Florida's red tides. *Geophysical Research Letters* 33, L11601, <http://dx.doi.org/10.1029/2005GL025449>.
- Hutchinson, G.E., 1965. The ecological theater and the evolutionary play. Yale University Press, pp 1–139.
- Ji, R., Chen, C., Franks, P.J.S., Townsend, D.W., Durbin, E.G., Beardsley, R.C., Lough, R.G., Houghton, R.W., 2006. Spring phytoplankton bloom and associated lower trophic level food web dynamics on Georges bank: 1-D and 2-D model studies. *Deep Sea Research Part II* 53, 2656–2683.
- Jochens, A.E., Nowlin, W.D., 1999. Northeastern Gulf of Mexico Chemical Hydrography and Hydrography Study. Annual Report: Year 2. OCS Study MMS 99-0054, New Orleans, LA, pp. 1–123.
- Jolliff, J.K., Walsh, J.J., He, R., Weisberg, R.H., Stovall-Leonard, A., Conmy, R., Coble, H.E., Nababan, B., Zhang, H., Hu, C., Muller-Karger, F.E., 2003. Dispersal of the Suwannee River plume over the West Florida shelf: simulation and observation of the optical and biochemical consequences of a “flushing event”. *Geophysical Research Letters*, 30, <http://dx.doi.org/10.1029/2003GL016964>.
- Jolliff, J.K., 2004. The Relative Influence of Coastal Effluent and Deep Water Masses on Surface Optical Signals and Margin Productivity in the Northeastern Gulf of Mexico: a Three-dimensional Simulation Analysis with Implications for the West Florida Shelf Plume. Ph.D. Dissertation. University of South Florida, Tampa.
- Jolliff, J.K., Kindle, J.C., Penta, B., Helber, R., Lee, Z., Shulman, I., Arnone, R., Rowley, C., 2008. On the relationship between satellite-estimated bio-optical and thermal properties in the Gulf of Mexico. *Journal of Geophysical Research, Biogeosciences* 113, G01024, <http://dx.doi.org/10.1029/2006JG000373>.
- Jurado, J.L., Hitchcock, G.L., Ortner, P.B., 2007. Seasonal variability in nutrient and phytoplankton distributions on the Southwest Florida inner shelf. *Bulletin of Marine Science* 80, 21–43.
- Kamatani, A., 1969. Regeneration of inorganic nutrients from diatom decomposition. *Journal of the Oceanographical Society of Japan* 25, 63–74.
- Kerfoot, J., Kirkpatrick, G., Lohrenz, S., Mahoney, K., Molene, M., Schofield, O., 2004. Vertical migration of a *Karenia brevis* bloom: implications for remote sensing of harmful algal blooms. In: Steidinger, K.A., Landsberg, J.H., Tomas, C.R., Vargo, G.A. (Eds.), *Harmful Algae 2002*. Florida Fish and Wildlife Commission, Florida Institute of Oceanography, and Intergovernmental Oceanographic Commission of UNESCO, St. Petersburg, FL, pp. 279–281.
- Kirchman, D.L., 1994. The uptake of inorganic nutrients by heterotrophic bacteria. *Microbial Ecology* 28, 255–271.
- Kirchman, D.L., 2000. Uptake and regeneration of inorganic nutrients by marine heterotrophic bacteria. In: Kirchman, D.L. (Ed.), *Microbial Ecology of the Oceans*. John Wiley & Sons, New York, pp. 261–289.
- Kleppel, G.S., Burkart, C.A., Carter, K., Tomas, C., 1996. Diets of calanoid copepods on the West Florida continental shelf: relationships between food concentration, food composition and feeding activity. *Marine Biology* 127, 209–218.
- Landsberg, J.H., 2002. The effects of harmful algal blooms on aquatic organisms. *Reviews in Fisheries Science* 10, 113–390.
- Lenes, J.M., Darrow, B.P., Cattrell, C., Heil, C.A., Vargo, G.A., Callahan, M., Byrne, R.M., Prospero, J.M., Bates, D.E., Fanning, K.A., Walsh, J.J., 2001. Iron fertilization and the *Trichodesmium* response on the West Florida shelf. *Limnology and Oceanography* 46, 1261–1277.
- Lenes, J.M., Walsh, J.J., Otis, D.B., Carder, K.L., 2005. Iron fertilization of *Trichodesmium* off the west coast of Barbados: a one-dimensional numerical model. *Deep Sea Research* 52, 1021–1041.
- Lenes, J.M., Darrow, B.A., Walsh, J.J., Prospero, J.M., He, R., Virmani, J., Weisberg, R.H., Vargo, G.A., Heil, C.A., 2008. Saharan dust and phosphatic fidelity: a three dimensional biogeochemical model of *Trichodesmium* as a nutrient source for red tides on the West Florida shelf. *Continental Shelf Research* 28, 1091–1115.
- Lenes, J.M., Heil, C.A., 2010. A historical analysis of the potential nutrient supply from the N₂ fixing marine cyanobacterium *Trichodesmium* spp. to *Karenia brevis* in the eastern Gulf of Mexico. *Journal of Plankton Research*, <http://dx.doi.org/10.1093/plankt/fbq061>.
- Lester, K.M., 2005. The Mesozooplankton of the West Florida Shelf: Relationships with *Karenia brevis* Blooms. Ph.D. Dissertation. University of South Florida, Tampa.
- Lester, K.M., Heil, C.A., Neely, M.B., Spence, D.N., Murasko, S., Hopkins, T.L., Sutton, T.T., Burghart, S.E., Bohrer, R.E., Remsen, A.W., Vargo, G.A., Walsh, J.J., 2008. Zooplankton and *Karenia brevis* in the Gulf of Mexico. *Continental Shelf Research* 28, 99–111.
- Masserini, R.T., Fanning, K.A., 2000. A sensor package for the simultaneous determination of nanomolar concentrations of nitrite, nitrate, and ammonia in seawater by fluorescence detection. *Marine Chemistry* 68, 323–333.
- McPherson, B.F., R.L. Miller, and Y.E. Stoker. 1996. Physical, Chemical, and Biological Characteristics of the Charlotte Harbor Basin and Estuarine System in Southwestern Florida: A Summary of the 1982–1989 U.S. Geological Survey Charlotte Harbor Assessment and Other Studies. U.S. Geological Survey Water-Supply Paper 2486. U.S. Geological Survey, Information Service, Denver, pp 1–32.
- Mellor, G.L., Yamada, T., 1982. Development of a turbulence closure model for geophysical fluid problems. *Reviews of Geophysics and Space Physics* 20, 851–875.
- Milroy, S.P., Dieterle, D.A., He, R., Kirkpatrick, G.J., Lester, K.L., Steidinger, K.A., Vargo, G.A., Walsh, J.J., Weisberg, R.H., 2008. A three-dimensional biophysical model of *Karenia brevis* dynamics on the West Florida shelf: a preliminary look at physical transport and zooplankton grazing controls. *Continental Shelf Research* 28, 112–136.
- Mulholland, M.R., Heil, C.A., Bronk, D.A., O'Neil, J.M., Bernhardt, P.W., 2004. Does nitrogen regeneration from the N₂ fixing cyanobacteria *Trichodesmium* spp. fuel *Karenia* blooms in the Gulf of Mexico? In: Steidinger, K.A., Landsberg, J.H., Tomas, C.R., Vargo, G.A. (Eds.), *Harmful Algae 2002*. Florida Fish and Wildlife Commission, Florida Institute of Oceanography, and Intergovernmental Oceanographic Commission of UNESCO, St. Petersburg, FL, pp. 47–49.
- Mulholland, M.R., Bernhardt, P.W., Heil, C.A., Bronk, D.A., O'Neil, J.M., 2006. Nitrogen fixation and release of fixed nitrogen by *Trichodesmium* spp. in the Gulf of Mexico. *Limnology and Oceanography* 51, 1762–1776.
- Nelson, J.R., Eckman, J.E., Robertson, C.Y., Marinelli, R.L., Jahnke, R.A., 1999. Benthic microalgal biomass and irradiance at the sea floor on the continental shelf on the South Atlantic Bight: spatial and temporal variability and storm effects. *Continental Shelf Research* 19, 477–505.
- O'Neil, J.M., Roman, M.R., 1992. Grazers and associated organisms of *Trichodesmium*. In: Carpenter, E.J., Capone, D.A., Rueter, J.G. (Eds.), *Marine Pelagic Cyanobacteria: Trichodesmium and other diazotrophs*. Kluwer Academic Publishers, the Netherlands, pp. 239–248.
- Pakulski, J.D., Benner, R., Whittedge, T.E., Amon, R.M.W., Eadie, B., Cifuentes, L.A., Ammerman, J., Stockwell, D., 2000. Microbial metabolism and nutrient cycling in the Mississippi and Atchafalaya River Plumes. *Estuarine Coastal and Shelf Science* 50, 173–184.
- Paul, J.H., Houchin, L., Griffin, D., Slifko, T., Guo, M., Richardson, B., Steidinger, K.A., 2002. A filterable lytic agent obtained from a red tide bloom that caused lysis of *Karenia brevis* (*Gymnodinium breve*) cultures. *Aquatic Microbiology Ecology* 27, 21–27.
- Phlips, E.J., Badylak, S., 1996. Spatial variability in phytoplankton standing crop and composition in a shallow inner-shelf lagoon, Florida Bay, Florida. *Bulletin of Marine Science* 58, 203–216.
- Qian, Y., Jochens, A.E., Kennicutt, M.C., Biggs, D.C., 2003. Spatial and temporal variability of phytoplankton biomass and community structure over the continental margin of the northeast Gulf of Mexico based on pigment analysis. *Continental Shelf Research* 23, 1–17.
- Roth, P.B., Twiner, M.J., Mikulski, C.M., Barnhorst, A.B., Doucette, G.J., 2008. Comparative analysis of two algalicidal bacteria active against the red tide dinoflagellate *Karenia brevis*. *Harmful Algae* 7, 682–691.
- Rueter, J.G., Ohki, K., Fujita, Y., 1990. The effect of iron nutrition on photosynthesis and nitrogen fixation in cultures of *Trichodesmium* (Cyanophyceae). *Journal of Phycology* 24, 30–35.
- Rueter, J.G., Hutchins, D.A., Smith, R.W., Unsworth, N.L., 1992. Iron nutrition of *Trichodesmium*. In: Carpenter, E.J., Capone, D.A., Rueter, J.G. (Eds.), *Marine Pelagic Cyanobacteria: Trichodesmium and Other Diazotrophs*. Kluwer Academic Publishers, the Netherlands, pp. 289–306.
- Sanudo-Wilhelmy, S.A., Kustka, A.B., Gobler, C.J., Hutchins, D.A., Yang, M., Lwiza, K., Burns, J., Capone, D.G., Carpenter, E.J., 2001. Phosphorus limitation of nitrogen fixation by *Trichodesmium* in the central Atlantic Ocean. *Nature* 411, 66–69.
- Saunders, R.P., Glenn, D.A., 1969. Diatoms. *Memoirs of the Hourglass Cruises Volume 1 (Part III)*, 1–119.
- Shchepetkin, A., McWilliams, J., 2005. The regional oceanic modeling system: a split-explicit, free-surface, topography-following-coordinate ocean model. *Ocean Modelling* 9, 347–404.
- Shimizu, Y., Wrensford, G., 1993. Peculiarities in the biosynthesis of brevitoxins and metabolism of *Gymnodinium breve*. In: Smayda, T.J., Shimizu, Y. (Eds.), *Toxic Phytoplankton Blooms in the Sea*. Elsevier, Amsterdam, pp. 919–923.
- Slobodkin, L.B., 1953. A possible initial condition for red tides off the coast of Florida. *Journal of Marine Research* 12, 148–155.
- Steidinger, K.A., Vargo, G.A., Tester, P.A., Tomas, C.R., 1998. Bloom dynamics and physiology of *Gymnodinium breve* with emphasis on the Gulf of Mexico. In: Anderson, D.M., Cembella, A.D., Hallegraeff, G.M. (Eds.), *Physiological Ecology of Harmful Algal Blooms*. Springer Verlag, Berlin, pp. 135–153.
- Stevenson, C., Childers, D.L., 2004. Hydroperiod and seasonal effects on fish decomposition in an oligotrophic Everglades Marsh. *Wetlands* 24, 529–534.
- Stihl, A., Sommer, U., Post, A.F., 2001. Alkaline phosphatase activities among populations of the colony-forming diazotrophic cyanobacterium *Trichodesmium* spp. (cyanobacteria) in the Red Sea. *Journal of Phycology* 37, 310–317.
- Stow, C.A., Jolliff, J., McGillicuddy Jr., D.J., Doney, S.C., Allen, J.L., Friedrichs, M.A.M., Rose, K.A., Wallhead, P., 2009. Skill assessment for coupled biological/physical models of marine systems. *Journal of Marine Systems* 76, 4–15.
- Strom, S.L., Strom, M.W., 1996. Microplankton growth, grazing, and community structure in the northern Gulf of Mexico. *Marine Ecology-Progress Series* 130, 229–240.
- Subramanian, A., Carpenter, E.J., Falkowski, P.G., 1999. Bio-optical properties of the marine diazotrophic cyanobacteria *Trichodesmium* spp. II. A reflectance model for remote sensing. *Limnology and Oceanography* 44, 618–627.
- Sutton, T., Hopkins, T., Remsen, A., Burghart, S., 2001. Multisensor sampling of pelagic ecosystem variables in a coastal environment to estimate zooplankton grazing impact. *Continental Shelf Research* 21, 69–87.
- Tester, P.A., Turner, J.T., Shea, D., 2000. Vectorial transport of toxins from the dinoflagellate *Gymnodinium breve* through copepods to fish. *Journal of Plankton Research* 22, 47–62.
- Thingstad, T.F., Strand, E., Larsen, A., 2010. Stepwise building of plankton functional type (PFT) models: a feasible route to complex models? *Progress in Oceanography* 84, 6–15.
- Turner, J.T., Tester, P.A., 1997. Toxic marine phytoplankton, zooplankton grazers, and pelagic food webs. *Limnology and Oceanography* 42, 1203–1214.

- Van Dolah, F.M., Lidie, K.B., Monroe, E.A., Bhattacharya, D., Campbell, L., Doucette, G.S., Kamykowski, D., 2009. The Florida red tide dinoflagellate *Karenia brevis*: new insights into cellular and molecular processes underlying bloom dynamics. *Harmful Algae* 8, 562–572.
- Vargo, G.A., Howard-Shablott, D., 1990. Phosphorus requirements in *Ptychodiscus brevis*: cell phosphorus, uptake and growth requirements. In: Graneli, E., et al. (Eds.), *Toxic Marine Phyto-plankton*. Elsevier, Amsterdam, pp. 324–329.
- Vargo, G.A., Heil, C.A., Ault, D.N., Neely, M.B., Murasko, S., Havens, J., Lester, K.M., Dixon, K., Merkt, R., Walsh, J.J., Weisberg, R.H., Steidinger, K.A., 2004. Four *Karenia brevis* blooms: a comparative analysis. In: Steidinger, K.A., Landsberg, J.H., Tomas, C.R., Vargo, G.A. (Eds.), *Harmful Algae 2002*. Florida Fish and Wildlife Commission, Florida Institute of Oceanography, and Intergovernmental Oceanographic Commission of UNESCO, St. Petersburg, FL, pp. 14–16.
- Vargo, G.A., Heil, C.A., Fanning, K.A., Dixon, L.K., Neely, M.B., Lester, K.A., Ault, D., Murasko, S., Havens, J.A., Walsh, J.J., Bell, S., 2008. Nutrient availability in support of *Karenia brevis* blooms on the central West Florida shelf: what keeps *Karenia* blooming? *Continental Shelf Research* 28, 73–98.
- Villareal, T.A., Carpenter, E.J., 1990. Diel buoyancy regulation in the marine diazotrophic cyanobacterium *Trichodesmium thiebautii*. *Limnology and Oceanography* 35, 1832–1837.
- Walsby, A.E., 1978. The properties and buoyancy providing role of gas vesicles in *Trichodesmium ehrenbergi*. *British Phycological Journal* 12, 103–116.
- Walsby, A.E., 1992. The gas vesicles and buoyancy of *Trichodesmium*. In: Carpenter, E.J., Capone, D.G., Reuter, J.G. (Eds.), *Marine Pelagic Cyanobacteria: Trichodesmium and Other Diazotrophs*. Springer, New York, pp. 141–161.
- Walsh, J.J., 1976. Herbivory as a factor in patterns of nutrient utilization in the sea. *Limnology and Oceanography* 21, 1–13.
- Walsh, J.J., Whittedge, T.E., Barvenik, F.W., Wirick, C.D., Howe, S.O., Esaias, W.E., Scott, J.T., 1978. Wind events and food chain dynamics within the New York Bight. *Limnology and Oceanography* 23, 659–683.
- Walsh, J.J., 1983. Death in the sea: enigmatic phytoplankton losses. *Progress in Oceanography* 12, 1–86.
- Walsh, J.J., Dieterle, D.A., 1994. CO₂ cycling in the coastal ocean. I. A numerical analysis of the southeastern Bering Sea, with applications to the Chukchi Sea and the northern Gulf of Mexico. *Progress in Oceanography* 34, 335–392.
- Walsh, J.J., Steidinger, K.A., 2001. Saharan dust and Florida red tides: the cyanophyte connection. *Journal of Geophysical Research* 106, 11597–11612.
- Walsh, J.J., Penta, B., Dieterle, D.A., Bissett, W.P., 2001a. Predictive ecological modeling of harmful algal blooms. *Human and Ecological Risk Assessment* 7, 1369–1383.
- Walsh, J.J., Dieterle, D.A., Lenes, J.M., 2001b. A numerical analysis of carbon dynamics of the Southern Ocean phytoplankton community: the roles of light and grazing in effecting both sequestration of atmospheric CO₂ and food availability to larval krill. *Deep Sea Research* 48, 1–48.
- Walsh, J.J., Haddad, K.A., Dieterle, D.A., Weisberg, R.H., Li, Z., Yang, H., Muller-Karger, F.E., Heil, C.A., Bissett, W.P., 2002. A numerical analysis of landfall of the 1979 red tide of *Karenia brevis* along the west coast of Florida. *Continental Shelf Research* 22, 15–38.
- Walsh, J.J., Weisberg, R.H., Dieterle, D.A., He, H., Darrow, B.P., Jolliff, J.K., Lester, K.M., Vargo, G.A., Kirkpatrick, G.J., Fanning, K.A., Sutton, T.T., Jochens, A.E., Biggs, D.C., Nababan, B., Hu, C., Muller-Karger, F.E., 2003. The phytoplankton response to intrusions of slope water on the West Florida shelf: models and observations. *Journal of Geophysical Research* 108, 3190, <http://dx.doi.org/10.1029/2002JC001406>.
- Walsh, J.J., Steidinger, K.A., 2004. ECOHAB:Florida — a catalyst for recent multi-agency studies of the West Florida shelf. In: Steidinger, K.A., Landsberg, J.H., Tomas, C.R., Vargo, G.A. (Eds.), *Harmful Algae 2002*. Florida Fish and Wildlife Commission, Florida Institute of Oceanography, and Intergovernmental Oceanographic Commission of UNESCO, St. Petersburg, FL, pp. 519–521.
- Walsh, J.J., Jolliff, J.K., Darrow, B.P., Lenes, J.M., Milroy, S.P., Remsen, A., Dieterle, D.A., Carder, K.L., Chen, F.R., Vargo, G.A., Weisberg, R.H., Fanning, K.A., Muller-Karger, F.E., Shinn, E., Steidinger, K.A., Heil, C.A., Prospero, J.P., Lee, T.N., Kirkpatrick, G.J., Whittedge, T.E., Stockwell, D.A., Tomas, C.S., Villareal, T.A., Jochens, A.E., Bontempi, P.S., 2006. Red tides in the Gulf of Mexico: where, when, and why. *Journal of Geophysical Research* 111, C11003, <http://dx.doi.org/10.1029/2004JC002813>.
- Walsh, J.J., Kirkpatrick, G.J., 2008. Ecology and oceanography of harmful algal blooms in Florida. *Continental Shelf Research* 28, 1–214.
- Walsh, J.J., Weisberg, R.H., Lenes, J.M., Chen, F.R., Dieterle, D.A., Zheng, L., Carder, K.L., Vargo, G.A., Havens, K.A., Peebles, E., Hollander, D.J., He, R., Heil, C.A., Mahmoudi, B., Landsberg, J.H., 2009. Isotopic evidence for dead fish maintenance of Florida red tides, with implications for coastal fisheries over both source regions of the West Florida shelf and within downstream waters of the South Atlantic Bight. *Progress in Oceanography*, 70, <http://dx.doi.org/10.1015/j.pocean.2008.12.005>.
- Walsh, J.J., Tomas, C.R., Steidinger, K.A., Lenes, J.M., Chen, F.R., Weisberg, R.H., Zheng, L., Landsberg, J.H., Vargo, G.A., Heil, C.A., 2011a. Imprudent fishing harvests and consequent trophic cascades on the West Florida shelf over the last half century: a harbinger of increased human deaths from paralytic shellfish poisoning along the southeastern United States, in response to oligotrophication??. *Continental Shelf Research*, <http://dx.doi.org/10.1016/j.csr.2011.02.007>.
- Walsh, J.J., Dieterle, D.A., Chen, F.R., Maslowski, W., Cassano, J.J., Whittedge, T.E., Stockwell, D., Flint, M., Sukhanova, I.N., Christensen, J., 2011b. Trophic cascades and future harmful algal blooms within ice-free Arctic Seas north of Bering Strait: a simulation analysis. *Progress in Oceanography*, <http://dx.doi.org/10.1016/j.pocean.2011.02.001>.
- Walsh, J.J., J.M. Lenes, B.P. Darrow, and F.R. Chen. 2011c. Forecasting and Modeling of Harmful Algal Blooms in the Coastal Zone. In: "Volume 9 of the Treatise on Estuarine and Coastal Science". Baird D. and Mehta A. (Eds.). Elsevier, Ch. 9.12, pp. 217–330.
- Weisberg, R.H., Li, Z., Muller-Karger, F.E., 2001. West Florida shelf response to local wind forcing. *Journal of Geophysical Research* 106, 31239–31262.
- Weisberg, R.H., He, R., 2003. Local and deep-ocean forcing contributions to anomalous water properties on the West Florida continental shelf. *Journal of Geophysical Research* 108, 3184, <http://dx.doi.org/10.1029/2002JC001407>.
- Weisberg, R.H., Barth, A., Alvera-Azcárate, A., Zheng, L., 2009. A coordinated coastal ocean observing and modeling system for the West Florida Shelf. *Harmful Algae* 8, 585–598.
- Yentsch, C.M., Yentsch, C.S., Perras, J.P., 1972. Alkaline phosphatase activity in the tropical marine blue-green alga *Oscillatoria erythraea* ('*Trichodesmium*'). *Limnology and Oceanography* 17, 772–774.
- Young, L., Christman, M., 2006. Analysis of *Karenia brevis* Gulf Data. Report to FWRI.